ELSEVIER

Contents lists available at ScienceDirect

Marine Pollution Bulletin

journal homepage: www.elsevier.com/locate/marpolbul





Modeling pollutant dispersion scenarios in high vessel-traffic areas of the Lower Amazon River

Alan Cavalcanti Da Cunha ^{a,*}, Carlos Henrique Medeiros De Abreu ^b, Jonathan Luz Pires Crizanto ^c, Helenilza Ferreira Albuquerque Cunha ^d, Alaan Ubaiara Brito ^e, Newton Narciso Pereira ^f

- ^a Civil Engineering Department, Federal University of Amapá, Graduate Program in Tropical Biodiversity (PPGBIO), Graduate Program in Environmental Sciences (PPGCA). Rodovia Juscelino Kubitschek de Oliveira, Km 02, 68902-280 Macapá, AP, Brazil
- ^b Graduate Program in Biotechnology (Bionorte), Federal University of Amapá, Rodovia Juscelino Kubitschek de Oliveira, Km 02, 68902-280 Macapá, AP. Environmental Engineering School (CEAM), Amapá State University (UEAP), Macapá-AP, 68900-070, Brazil.
- c Graduate Program in Tropical Biodiversity (PPGBIO), Federal University of Amapá, Rodovia Juscelino Kubitschek de Oliveira, Km 02, 68902-280 Macapá, AP, Brazil
- d Environment and Development Department, Federal University of Amapá, Graduate Program in Tropical Biodiversity (PPGBIO), Graduate Program in Environmental Sciences (PPGCA). Rodovia Juscelino Kubitschek de Oliveira, Km 02, 68902-280 Macapá, AP, Brazil
- ^e Electrical Engineering Department, Federal University of Amapá, Graduate Program in Environmental Sciences (PPGCA). Rodovia Juscelino Kubitschek de Oliveira, Km 02, 68902-280 Macapá, AP, Brazil
- ^f Production Engineering Department, Industrial and Metallurgical Engineering School of Volta Redonda, Federal Fluminense University, Av. dos Trabalhadores 420 Sala C77 Vila Sta. Cecília, 27255-125 Volta Redonda, RJ, Brazil

ARTICLE INFO

Keywords: Scenarios Littoral Sensitivity Index Amazon Estuary Environmental impacts Accident prevention

ABSTRACT

Large ships are efficient in transporting oil and its derivatives. However, they can cause spills in the event of accidents. The aim of the study is to simulate oil dispersion processes in scenarios of likely accidents with ships traveling on sea routes interconnected with Amazonian ports and with the Atlantic Ocean. Navigation routes were based on traffic data to identify risk areas, as well as to compare them to data from the environmental (oil) sensitivity index and to results of numerical simulations of plumes dispersion. These three approaches were integrated to each other in order to assess potential environmental impacts of plumes on coastal biota and human populations. Scenarios results have indicated that the rainy season is the most critical period for plumes dispersion. But, depending on the emission point, plumes tend to remain close to the coast, extend up to 132 km within 72 h, affecting the biodiversity, protected areas and water supply systems from the urban areas.

1. Introduction

Oil tankers account for approximately 28% of the world fleet. Although they are efficient in transporting oil, they can cause oil spills in the event of accidents. Damage caused by accidents can lead to oil spills, damage ships' structure, as well as lead to the degradation of maritime and river environments, explosions, traffic blockages and permanent damage to ships (Calle and Alves, 2011; Uğurlu et al., 2015).

Therefore, ships navigating at sea and estuaries do not have absolute operation safety because the risk of accidents is a constant reality, either during extraction processes or during the transportation of crude oil or its derivatives (Lopes et al., 2009; Xu and Wang, 2014). For example,

ship collisions account for most maritime and estuarine accidents; the risk may be even higher in ports presenting high traffic density or complex bathymetric conditions (Yoo and Kim, 2019). In addition, vessel traffic features may also differ depending on maritime areas and routes; accident risk assessment mainly takes place in port areas, as indicated by Maritime Safety Audit (MSA) (Yoo and Kim, 2019). Large amounts of oil can be released in these restricted areas and reach vulnerable ecosystems and urban communities (Xu and Wang, 2014; Shi et al., 2019; Lu et al., 2017).

Despite this scenario, risk analysis at global level seems to show decreasing frequency of oil spills over time, which corresponded to 6.6/year in 2010. However, it also indicates growing trends to storage/

E-mail addresses: alancunha12@gmail.com (A.C. Da Cunha), chmabreu@gmail.com (C.H.M. De Abreu), jonathanluz3@gmail.com (J.L.P. Crizanto), helenilzacunha@gmail.com (H.F.A. Cunha), aubrito@unifap.br (A.U. Brito), newtonpereira@id.uff.br (N.N. Pereira).

^{*} Corresponding author.

refinery and gas pipeline spills, as well as to stationary spills associated with exploration/production processes, which corresponded to frequency value of 0.54/year in 2010 (Melaku Canu et al., 2015).

On the other hand, the overall risk of accidents in Brazilian waterways, such as the Amazon ones, increases due to the number of vessels using them to transport cargo and passengers. According to the Brazilian Navy Communication Center, there were 832,717 vessels registered in 2015; this number has increased to 859,852 and 877,692 in 2016 and 2017, respectively (EBC, 2017).

In fact, the country has recorded several accidents with vessels involving both inland (62%) and open sea (38%) navigation (Marinha do Brasil, 2019). For example, small vessels navigating in Amazonian rivers often experience stability or watertightness issues; besides, they are more susceptible to accidents in free-flowing rivers (Pereira, 2007; Padovezi, 2012). In addition, vessels facing adverse climatic conditions can be adjunct factors to risky environments for river transportation (Santos, 2013). Based on the operational perspective, malpractice and human errors tend to increase the risk of accidents involving vessels sailing on Brazilian rivers (Padovezi, 2012). Thus, accidents take place due to physical and environmental features of waterways and to vessels' poor behavior and operation process (Yoo and Kim, 2019).

Vessels navigating in the open sea often experience fewer accidents, since they are equipped with electronic navigation assistance systems and present better-quality stability and navigation projects that give them greater ability to react to adverse events. These are the reasons why the 2002 Maritime Transportation Security Act has established requirements for tracking vessels in order to improve the national security of the United States; the aforementioned Act has made it mandatory installing the Automatic Identification System (AIS) in American waters. The AIS on board ships transmits information such as vessel name, position, speed and course. In addition, receivers at destination are sent data made available by AIS in open sea areas, in inland waters and in ports (Mou et al., 2010). At the same time, there was widespread increase in the use of systems such as ARPA (Automatic Radar Plotting Aids), GMDSS (Global Maritime Distress & Safety System), GPS (Global Positioning System) and ECDIS (Electronic Chart Display and Information System) in global navigation (Xu and Wang, 2014).

Thus, significant changes were observed in Amazonian river ports due to international maritime trade and cabotage in the last twenty years, as well as to the emergence of larger ships (maximum 50 thousand tons); these changes have turned ship maneuvers into an even harder task, not to mention that the number of crew members tends to decrease, which makes this challenge even more complex for navigators (Pereira et al., 2014). On the other hand, despite these safety mechanisms, according to navigation records of ships sailing in the Lower Amazon River (AIS), there has been considerable frequency of ships traveling above the maximum speed allowed on the waterway (> 40%), i.e., faster than 10 knots. However, they can often reach up to 15 knots (30% of records), which can considerably increase the risk of accidents (Fragoso-Neto et al., 2018).

Environmental sensitivity index (ESI) mappings of the entire Brazilian coastal zone, with emphasis on the area comprising the Amazon River estuary, are available (IEPA, 2016; IEPA, 2017). ESI mappings are tools used to plan contingency and response actions in oil-related accidents (Zamboni et al., 2004). Thus, they are mandatory requirements for several environmental licensing processes (Marinho, 2012). It is necessary determining the Littoral Sensitivity Index (LSI) for each coastline segment in order to make these mappings. This index is based on geomorphological, hydrodynamic and biological features of the area, which are used to determine its environmental sensitivity degree (Gil-Agudelo et al., 2015). Therefore, the use of LSI maps can vary from coast protection and cleaning planning (in specific places) to strategic planning for contexts of major accidents in remote areas at regional scale (Zamboni et al., 2004; de Andrade et al., 2018).

LSI maps of Amazonas River Mouth Basin region have not yet been

tested in simulations of accidental spill of oil, or oil derivatives, in risky situations (Fig. 1). Thus, it is essential developing operational/tactical strategies to be applied in the event of accidents in order to optimize preventive actions, minimize likely damage and guarantee the protection of vulnerable natural resources and local communities, including potentially-affected protected areas and urban zones (Macapá and Santana cities and Port Area) (Ward et al., 2013; Mancio Filho, 2014; Dias et al., 2016; IEPA, 2017; Santos et al., 2018; Abreu et al., 2020).

The aim of the present research was to numerically simulate the dispersion of hypothetical oil plumes in areas identified as presenting higher risk of collision or accidents between vessels traveling in the Amazon River Estuary (AIS), based on a hydrodynamic and environmental modeling system (SisBaHia) (Rosman, 2018) and on a previous knowledge base of currents observed in the region (Abreu et al., 2020).

Four (4) specific sites were identified as potential areas for oil spill accidents in the Amazon River estuary. The identification process was based on statistical data - such as route and intensity - provided by the Automatic Identification System (AIS) about the ship traffic taking place in these critical waterway sections from 2016 to 2019 (Fig. 1). Therefore, it was possible mapping the places most likely susceptible to oil spills, as well as estimating the extent and concentration of pollutant plumes based on a given hydrological period (Abreu et al., 2020), on the distance from the accident point to the coast and to the waterway route, as well as on the most likely distance from the banks of the Amazon River and the corresponding LSI value (IEPA, 2016). In addition, S500 diesel oil was selected as the pollutant most likely to be spilled, since it is the oil type mostly transported by ships in the Amazon region.

All four scenarios used for pollutant dispersion modeling and simulation purposes were applied to two hydrological times (rainy season - May / dry season - November) by taking into consideration the hydrodynamic and climatic features representative of Amazonian coastal ecosystems (bathymetry, tidal phase and amplitude, flow, current speed, temperature and wind effect). Results recorded for these scenarios were compared to LSI and AIS data.

2. Materials and methods

2.1. Study site and period

The mouth of the Amazonian Maritime Basin is located at the Northern end of the Brazilian coast (Fig. 1). Based on the environmental viewpoint, Amapá (0°02′06″ S; 51°10′30″ W) and Pará states (1°26′35″ S; 48°29′51″ W), as well as part of Maranhão State (2°33′38″ S; 44°21′44″ W), cover the Brazilian Amazon coast, which presents a variety of fragile coastal and marine ecosystems that extend from São Marcos Bay to Orinoco River Delta in Venezuela; these ecosystems are directly influenced by the Amazon River Dispersion System (IEPA, 2016).

The Estuarine Coast of Amapá (ECA) State is in direct contact with the Northern Amazon River Channel and presents clay and silt substrate along the flooded plain of the Amazon River and of its tributaries; it is also influenced by micro, *meso* and macro tides (Torres et al., 2018). The inner part of the Amazon River mouth and the mangroves give way to extensive low plains and flooded forests that cover the substrate of river and island banks, as well as of flood plains. Small beaches can be seen on the internal estuarine coast, close to Macapá and Santana cities (IEPA, 2017).

This coast presents the largest continuous mangrove areas world-wide, as well as the largest coastal marshes in Brazil. The location of this coastline in the tropical equatorial region and its regional geological/geomorphological, oceanographic, climatological and hydrographic features enable the incidence of high magnitude and amplitude driving forces (Abreu et al., 2020; Torres et al., 2018; Valerio et al., 2018).

Estuarine semidiurnal tides, with local amplitudes of up to 3–4 m (and up to 12 m on the ocean coast), present strong currents perpendicular to the coast. The seasonal displacement of the Intertropical

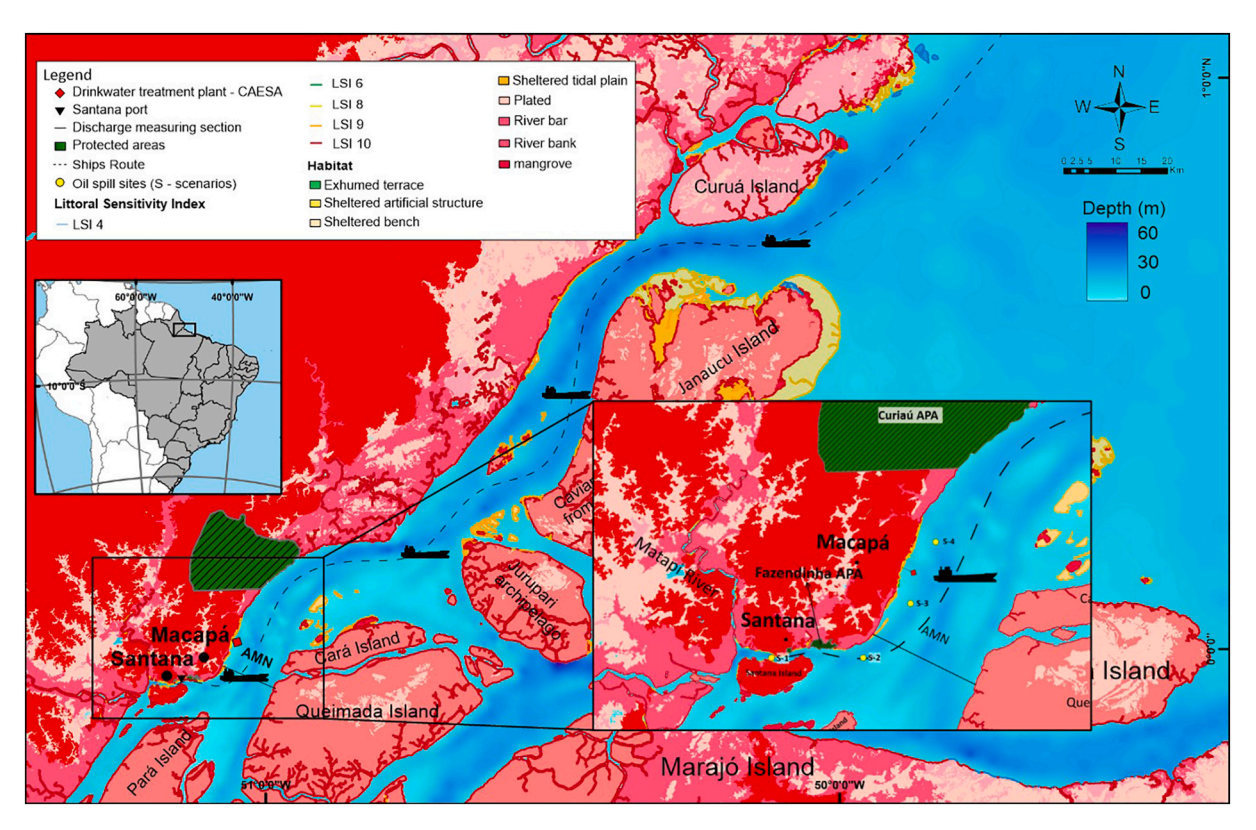


Fig. 1. Critical estuarine zone of Amapá State coast (Macapá and Santana cities) and Protected Areas (green spot). The vessel monitoring area is defined based on the most intense traffic (black dotted line). Coastline colors represent the Littoral Sensitivity Index (LSI). S is representative of the place most susceptible to oil spill. S-1 = Port of Santana; S-2 = Santana Channel; S-3 = Pedrinhas River Mouth; and S-4 = CAESA (water treatment unit). Source: Adapted from IEPA (2017). (For interpretation of the references to colour in this figure legend, the reader is referred to the web version of this article.)

Convergence Zone (ICZ) results in constant river breeze action and influences wave generation (Kuhn et al., 2010; Gallo and Vinzon, 2005). The massive flow (210 thousand m³ s -1) of the Amazon River is capable of transporting thousands of tons of sediments to the ocean along the coast towards Venezuela (Gallo and Vinzon, 2015). The action of these driving forces results in coastal morphology under constant changes (Torres et al., 2018; IEPA, 2017; Santos et al., 2018), which increases the complexity of fuel storage, transportation and transshipment operations. However, there is lack of contingency plans, which makes it essential conducting studies focused on stopping and/or mitigating likely environmental disasters involving oil and oil-derivative spills (Cunha et al., 2012).

The most intense vessel traffic is indicated by a black dotted line (Fig. 1). It is the technical justification for the present research, due to its regional economic importance and mainly because it corresponds to the geographical domain for the mandatory entry and exit route of ships used to sell Brazilian goods and exports (UNCTAD, 2008).

This region is environmentally sensitive when it comes to the coastal aquatic biota, besides hosting protected areas and several riverside communities. Therefore, it is relevant for Amazonian biodiversity conservation and preventive protection against likely catastrophic episodes involving potential accidents with ships (IEPA, 2017). Fig. 1 shows the Littoral Sensitivity Indices (LSI), different habitats and most likely sites for potential oil spills (S-1, S-2, S-3 and S-4). The red diamond in the legend represents the Water Treatment Station (CAESA or S-2) in Macapá City, between S-3 and S-4. Black dots represent the two main cities in Amapá State, namely: Macapá and Santana. Port of Macapá, also known as Port of Santana Docks, is located in Santana City. Fazendinha Environmental Protection Area (Gazendinha EPA) and Curiaú Environmental Protection Area (Curiaú EPA) - highlighted in green on the map – are located close to Macapá and Santana cities, respectively.

2.2. Climate data

Climatic features of the investigated region show high rainfall rates (\approx 2300 mm/year), high temperature (never below 18 °C) and significantly sharp dry season (August to November); the climate in the region is classified as Am (monsoon climate), based on Köppen's methodology (Köppen, 2020). Climatic variation takes place in two main periods, namely: the Amazon rainy season, from January to August, which presents the highest rainfall rate between March and May; and the least rainy period in the Amazon region, from September to November (Limberger and Silva, 2016; Marengo and Espinoza, 2016; De Souza et al., 2017).

Wind intensity variation are similarly seasonal, although opposed to rainfall events (Kuhn et al., 2010). Wind speed is lower in the rainiest period and faster in the lesser rainy period (higher intensity). Meteorological data recorded for rainfall in the present study are ≈ 400 mm and ≈ 60 mm in May and November, respectively. Wind intensity lies within the following intervals: $[0 \le V_{(Air)} \le 2 \text{ m s}^{-1}]$ in May and $[1 \le V_{(Air)} \le 3 \text{ m s}^{-1}]$ in November. These intervals were based on an 8-year-long time series (2010–2018) made available by Macapá meteorological station (MACAPA-AP-OMM: 82098), which is close to Fazendinha EPA. Data were provided by the Meteorological Database for Teaching and Research-BDMEP of the Brazilian National Institute of Meteorology (Instituto Nacional de Meteorologia - INMET).

2.3. AIS data collection

The risk of accidents can be defined as the likelihood of an unwanted event to take place multiplied by the consequences of this event (Marignani et al., 2017). Risk assessment lies on comparing the risk analysis results to risk criteria in order to assess likely actions to be taken, or whether the observed risks are acceptable or not. One, or more, actions

should be adopted and implemented during the analysis stage to help mitigating these risks (Xu and Wang, 2014).

Traffic data was generated in automated tracking system used on ships, as well as by Vessel Traffic Services (VTS) used to identify and locate vessels and telemetrically exchange data with other ships and stations nearby (Montewka et al., 2010; Pereira et al., 2014). The system can automatically transmit the position and speed of ships, among other information, to an AIS data receiver. The International Convention of the International Maritime Organization for the Safety of Life at Sea (SOLAS) requires AIS to be installed on board of ships making international trips with gross tonnage (GT) of 300 t, or more, as well as on board of all passenger ships, regardless of size (Mou et al., 2010).

AlS data are used as source of information to help determining ships' route between port terminals and maritime/estuarine traffic routes, as well as to identify and estimate risks associated with navigation on waterways (Van Dorp and Merrick, 2011; Pedersen, 1995). Data collected during the monitoring of ships navigating in AMN (Northern Channel close to Macapá City) enables making several analyses of monitored variables such as ship type and speed in "knots", ports of origin and destination, ship flag, construction year, length (m) and width (m), as well as geographic position (latitude/longitude), date and time of registration (Pereira et al., 2014). For example, these data were specifically collected for the period between March 14, 2016 and March 14, 2019; they also included indicators such as physical features and frequency of ships sailing in the investigated region (Pereira et al., 2014; Fragoso-Neto et al., 2018).

2.3.1. Evaluating ship operation in the Amazon Basin

Features of ships circulating in the Northern Channel (AMN - Fig. 1) during the investigated period are shown in Table 1. Approximately 3917 vessels of different classes were monitored; 184 vessels were removed from the analysis due to lack of available DWT (deadweight tonnage) and speed data. These vessels belonged to different classes (Passenger, Pilot Vessel, Pleasure Craft and Offshore Supply Ship). Thus, the analysis has focused on the universe of 3733 ships, based on the identified classes of vessels, as well as on mean DWT and standard deviation.

Bulk carriers (a) accounted for 56% of the total number of analyzed vessels, whereas ships carrying oil (f, j, k, l and p) accounted for 11%. If one only takes into consideration ships carrying oil products, the mean DWT recorded for these classes is of the order of 36,522 t; they are limited by the maximum operational draft in Amazonian ports. This

Table 1
Ship features based on AIS data for DWT (tons).

Unit	Ship features	Number of ships	Mean DWT (tons) \pm (standard deviation)
a	Bulk Carrier	2120	$68,585 \pm 17.833$
b	CABU Carrier	14	72,562 \pm NA
c	Cargo	3	$78,312 \pm 2.914$
d	Cargo/containership	4	$49,\!591\pm 1.074$
e	Cement Carrier	48	$16{,}763 \pm 686$
f	Chemical tanker	39	$37,912 \pm 14.264$
g	Container ship	543	$41,196 \pm 9.726$
h	General cargo	64	$21,339 \pm 14.328$
i	LPG tanker	226	5522 ± 1.089
j	Offshore supply ship	1	$1930 \pm NA$
k	Oil products tanker	50	$46,201 \pm 5.815$
1	Oil/chemical tanker	279	$40,\!090\pm12.501$
m	Oil/chemical tanker (crude oil tanker)	2	$17{,}743 \pm 98$
n	Ore Carrier	169	$81,452 \pm 1.395$
0	Passenger ship	53	4103 + 2.010
	Passenger ship	4	3378 ± 2.444
p	Tanker	35	$40,664 \pm 13.347$
q		4	346 + NA
r	Tug	•	
S	Wood chips Carrier	75	$52,053 \pm 2.060$
	Total	3733	

restriction is applied to the Amazon River mouth, where the maximum operational draft of ships is 11.50 ± 0.2 m (Barra Norte, not shown in Fig. 1). Based on AIS data, it was possible seeing at least 3 ships/day sailing or circulating in the investigated area, where traffic speed in navigation operations, as well as piloting and anchoring time at Fazendinha, were computed.

Data collected in AIS have indicated that ships at zero speed (0) are those anchored and waiting for pilot support on board - 954 records, in total. Most ships were traveling at speed ranging from 12 to 15 knots. Ships traveling at the highest speed comprised bulk carriers (56%), containers (13%), oil tankers (12%), LPG tankers (9%), ores carriers (6%) and the remaining ones were distributed among other classes.

In total, 700 ships were traveling faster than 15 knots; they were mostly containers, bulk carriers, oil tankers, LPG tankers, among others. Since tankers transport flammable and combustible material and overall operate in the navigation channel within these speed ranges (Northern Channel), the risks of oil/oil-derivative spills in the event of an accident tend to increase among these classes.

The highest concentration of anchored ships was observed in the region close to Macapá City. However, Port of Santana presents greater risk of accidents due to difficulties associated with the maneuvering and traffic of other vessels where the channel is relatively narrow (\approx 500–700 m, S-1 site in Fig. 1). These places are likely to present higher risk of accidents, mainly with tankers, which accounted for approximately 228 of the observed vessels. The main Amazonian ports, such as Port of Santana, received the largest number of the aforementioned oil/chemical vessels, whereas Port of Macapá received the total number of 79 vessels in the investigated period.

Mean DWT recorded for these ships is approximately 42,212 t, whereas the standard deviation is 10,886 t. The mean derivative-product transport capacity of these ships is approximately 52,000 m³. The estimated volume of dangerous products transported by ships sailing in the region in the investigated period was of approximately 12,034,000 m³ (\approx 3,008,500 t/year, on average). If one only takes into consideration ships operating on the Brazilian coast, the traffic of origin and destination of these vessels (import and export, indicating the next destination port) comprises, in total, approximately 3094 (82%) vessels operating in Amazonian waters (Fig. 2).

The destination of ships indicated by AIS, whose origin was the Amazon basin itself (n = 948), was concentrated in Port of Santana. In addition, the number of ships at speed 0 has indicated the number of ships anchored at the port (n = 954).

2.3.2. Evaluation of Environmental Sensitivity Index (ESI) charts, Littoral Sensitivity Indices (LSI) and risks

ESI charts are environmental planning instruments used in the event of oil spill (IEPA, 2016). Thus, the risk area mapped in the current research is part of coastal environments in the Mouth of the Amazonian Maritime Basin. This basin extends from Pará State (Marajó Island, Brazil) to French Guiana; it provides a thematic and cartographic database that shows the sensitivity index of coastal environments (LSI or ESI charts). These charts are associated with environmental remediation and recovery degree after likely disasters. Thus, LSI indicates that the most sensitive environment is the one facing more difficulty to recover (IEPA, 2017; Mancio Filho, 2014).

Coastlines highlighted by the reddest shades are the most sensitive ones [$1 \le ISL \le 10$]. Most of them present high littoral sensitivity indices (LSI close to 9–10); scale 10 accounts for the highest sensitivity degree (MMA, 2004). Thus, ESI charts are international standard georeferencing tools used to help preventing environmental impacts; they are often applied in oil exploration areas (EPBR, 2020), as well as in areas susceptible to accidents caused by ship traffic (Ellis, 2011; Uğurlu et al., 2015; Lu et al., 2017).

Factors taken into consideration to classify the littoral environmental sensitivity (LSI) to oil spill comprise 1) level of exposure to wave and tidal energy, 2) coastal slope and 3) substrate type (MMA, 2004).

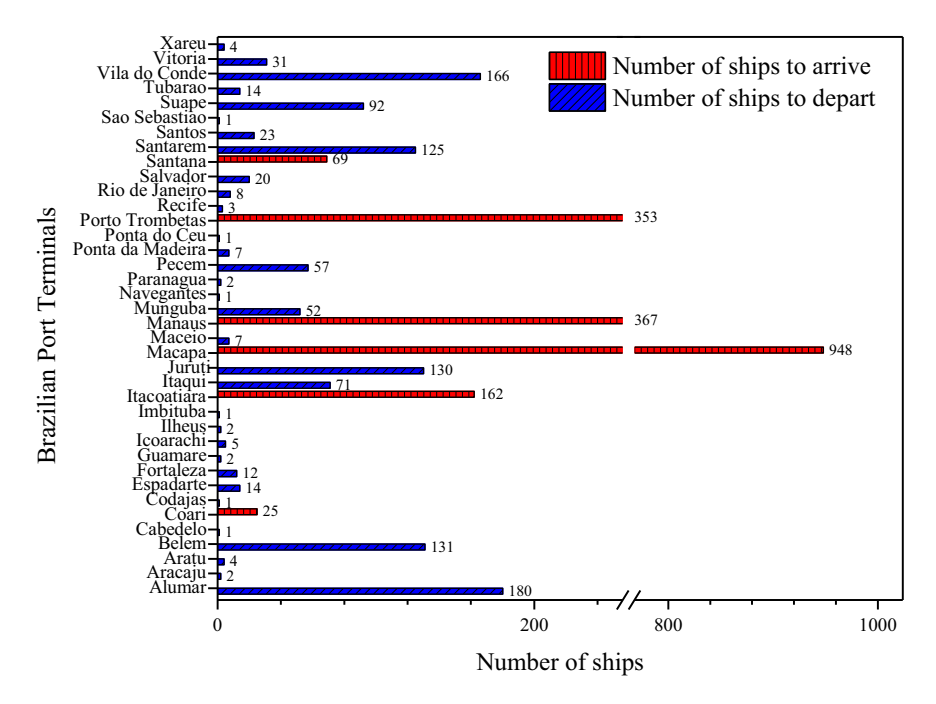


Fig. 2. Ship traffic in Port of Macapá and in other Brazilian ports.

However, biological aspects are also taken into consideration and integrated in the LSI. They are often associated with the production and biological sensitivity of coastal habitats, as well as with the geomorphology influencing the typology and density of biological communities and the diversity of these coastal systems (IEPA, 2016). So far, ESI charts were not tested in numerical simulations to assess the dispersion and extent of plumes deriving from hypothetical oil spills.

and Lagrangian models (pollutant dispersion) for transport phenomena (Rosman, 2018). The 2DH model (Eqs. (1)–(3)) was used to simulate the hydrodynamic behavior of the pollutant, whereas the Lagrangian model was used to simulate its dispersive process.

$$\frac{\partial U}{\partial t} + U \frac{\partial U}{\partial x} + V \frac{\partial U}{\partial y} = -g \frac{\partial \zeta}{\partial x} - \frac{gH}{2\rho_{\circ}} \frac{\partial \widehat{\rho}}{\partial x} + \frac{1}{H\rho_{\circ}} \left(\frac{\partial \left(H \widehat{\tau}_{xx} \right)}{\partial x} + \frac{\partial \left(H \widehat{\tau}_{xy} \right)}{\partial y} \right) + \frac{1}{H\rho_{\circ}} \left(\tau_{x}^{S} - \tau_{x}^{B} \right) - \frac{1}{H\rho_{\circ}} \left(\frac{\partial S_{xx}}{\partial x} + \frac{\partial S_{xy}}{\partial y} \right) + 2\Phi senV - \frac{U}{H} \Sigma q$$

$$(1)$$

$$\frac{\partial \mathbf{V}}{\partial t} + \mathbf{U}\frac{\partial \mathbf{V}}{\partial x} + \mathbf{V}\frac{\partial \mathbf{V}}{\partial y} = -\mathbf{g}\frac{\partial \zeta}{\partial y} - \frac{\mathbf{gH}}{2\rho_{\circ}}\frac{\partial \widehat{\rho}}{\partial x} + \frac{1}{H\rho_{\circ}}\left(\frac{\partial \left(\mathbf{H}\widehat{\tau}_{xy}\right)}{\partial x} + \frac{\partial \left(\mathbf{H}\widehat{\tau}_{xy}\right)}{\partial y}\right) + \frac{1}{H\rho_{\circ}}\left(\tau_{y}^{S} - \tau_{y}^{B}\right) - \frac{1}{H\rho_{\circ}}\left(\frac{\partial S_{yy}}{\partial y} + \frac{\partial S_{xy}}{\partial x}\right) - 2\Phi \operatorname{senU} - \frac{\mathbf{V}}{\mathbf{H}}\Sigma \mathbf{q}$$
(2)

2.4. Modeling and simulation

The information about oil spill defines the spill scenario. Thus, it is necessary to minimally include in the model the physical-chemical properties, schedule, location and start/end times of the spills (Spaulding, 1988). In addition, the definitions of wind fields, current and temperature in space and time are the initial parameters typical of hydrodynamic and environmental modeling processes (Abreu et al., 2020; Rosman, 2018; Cunha et al., 2012). They require high quality environmental data and must be carefully integrated in the dispersive oil spill model.

The SisBaHia software uses a 3D or 2DH hydrodynamic circulation model that is optimized for natural water bodies, in addition to Eurelian

$$\frac{\partial \zeta}{\partial t} + \frac{\partial UH}{Ux} + \frac{\partial VH}{\partial v} = \Sigma q \tag{3}$$

Wherein U is the speed on axis x (m s⁻¹); V is the speed on axis y (m s⁻¹); ζ represents the free elevation of the water surface (m); H is the water column depth (m); ρ_0 is the mean water density (kg m⁻³); ρ_r is the reference water density (kg m⁻³); g is the gravity acceleration (m s⁻²); τ_{ij} is the turbulent stress tensor; and (i, j) are the indices in the horizontal plane (x; y); τ_i i'S and τ_i i'B are the wind stress on the surface of the water and the lower friction stress, respectively (kg m⁻¹ s⁻²); 2Φ sen θ U and $2\Phi\theta$ senV represent the Coriolis accelerations, Φ is the angular speed of Earth's rotation (rad s⁻¹); θ is the latitude angle, $\sum q$ represents the

water balance based on atmospheric precipitation, infiltration and evaporation; and S_{ij} represents the effect of radiation stresses (Rosman, 2018; Cunha et al., 2006).

The 2DH hydrodynamic model takes into consideration the flow of "shallow" water that is noncompressible with the water density in the control volume of the fluid in motion. Contaminating sources in the Lagrangian model are represented by several particles launched in the source region, at regular time intervals. Particles randomly arranged in the source region are transported by the currents computed through the hydrodynamic model. The position of any particle at the following instant is defined by P^{n+1} , approximated by a second-order Taylor Series expansion, based on the previously known previous position of the particles (P^n) (Eq. (4)):

$$P^{n+1} = P^n + \Delta t \frac{dP^n}{dt} + \frac{\Delta t^2}{2!} \frac{d^2 P^n}{dt^2} + O^3 \tag{4} \label{eq:4}$$

With respect to effluents deriving from any source, the amount of mass (M_a) of a given species a observed in each particle when it enters the modeled domain is given by the following equation:

$$M_{a} = \frac{QC_{a} \times \Delta \tau}{N_{D}}$$
 (5)

Wherein Q is the effluent discharge from the source (m^3 s⁻¹), C_a is the concentration of the substance found in the source discharge (kg m^{-3}), and N_P is the number of particles entering the domain through the source at time step Δt (s). The dimensions of the source region are defined in such a way that the concentration in the source region is the same as that observed at the end of the initial dilution process, within the field close to the contaminant plume mix (Rosman, 2018).

2.4.1. First-order kinetic reactions of the Lagrangian model

According to the Lagrangian model, the total amount of contaminant (QT) released by a given source region at each time interval $\Delta\tau$ (Rosman, 2018) is given by:

$$QT = QQ/s \times \Delta \tau \tag{6}$$

Furthermore, it takes into consideration that, if NP particles are launched in each $\Delta \tau$, the initial quantity of each particle, m_0 , will be:

$$m_{o} = \frac{QT}{N_{P}} = \frac{QQ/s \times \Delta\tau}{N_{P}} \tag{7}$$

Assumingly, the amount remaining of each particle $m(t_v)$ over time is based on its life span t_v – i.e., it is possible specifying kinetic reactions $R(t_v)$ capable of changing the initial quantity of each particle, as follows:

$$m(t_{v}) = m_{o}R(t_{v}) \tag{8}$$

It is necessary taking into consideration evaporation-based losses, as well as specifying R (t_{ν}) and t_{ν} values in the Lagrangian model, for oil dispersion simulation purposes (Rosman, 2018). These values were obtained through the ADIOS2 (Automated Data Inquiry for Oil Spills)

mass loss model.

2.4.2. Boundary and initial conditions of the model

SisBaHiA can use two boundary condition groups, namely: closed boundary nodes can be used to impose water discharge values, whereas open boundary nodes can be used for free surface elevation values (Cunha et al., 2006). A series of water surface elevations was imposed at the open limit in order to represent tidal waves. Accordingly, the model was parameterized based on the six main tidal components (M_2 , S_2 , N_2 , K_1 , O_1 and M_4) imposed on nodes of the open boundary mesh. The closed limit was imposed on water discharged from the Amazon River (Óbidos station and experimental data in front of Port of Macapá, called Northen Channel of Macapá - CNM), as well as on two of its main tributaries (Xingu and Tapajós rivers). The boundaries at the lateral and bottom limits were considered impermeable and subjected to non-slip conditions. Constant elevation and speed values were used as initial condition; boundary conditions were generated from previous simulations conducted in SisBaHia itself (tidal flow, amplitude, intensity and wind speed direction; bathymetry, roughness and rainfall) (Abreu et al., 2020)

Data specifically associated with water flow were inserted in the model based on a measurement campaign carried out in the port area of Santana City (CSA) and in AMN between March 18–19, 2019. Experimental data available in the literature (Silva, 2009; Rosman, 2018) and data provided by the National Water Agency (ANA) of Óbidos station (code 00155001) were also used in the model. Rainfall, wind direction and intensity data were collected from the Meteorological Database for Teaching and Research-BDMEP of the Brazilian National Institute of Meteorology (INMET).

2.4.3. Fuel oil decay time - S500

S500 oil is the fuel mostly transported in the tanks of ships traveling in the Amazon region (Vieira et al., 2017). Its physical-chemical features are described in detail in the literature (Zanão et al., 2018; Toz et al., 2016; Peixoto et al., 2015; NOAA, 2000) and were included in the herein adopted dispersion model (Lagrangian).

The parameterization of the dispersion model was defined as follows: a) concentration at the launch site $C_0=102~mg~L^{-1};\,b)$ spill flow, $Q=0.2~m^3~s^{-1}$ (based on the flow of a single vessel with mean load of 50 thousand t); c) pollutant emission time after an accident, up to $T_{Lim}=72~h$ at a specific tidal stage and potential spillage site (scenarios S-1, S-2, S-3 or S-4); d) estimated imposition of pollutant decay (decomposition reaction kinetics): $K_{r(28oC)}=0.25~day^{-1}$ (ADIOS2), wherein the curve adopted as standard was that of Vol% (28 °C) (ADIOS 2) (Fig. 3); e) ebb flow in the Northern Channel of the Amazon River (CNA-Ebb) $Q=261,422~m^3~s^{-1}$ and flood flow Q (Northern Channel - Flood) $=-145,925~m^3~s^{-1}.$

Based on the previous assumptions, the decay curve estimated in the ADIOS2 Software (Zanão et al., 2018; Toz et al., 2016; Peixoto et al., 2015; Gurgel et al., 2018; NOAA, 2000) presented restricted

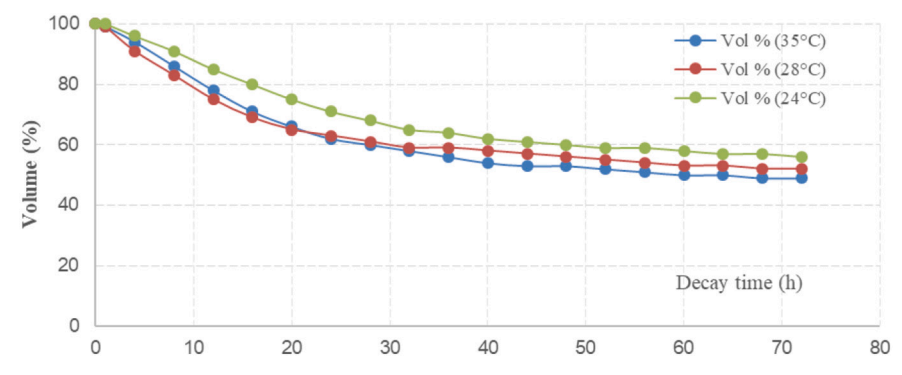


Fig. 3. Decay curves plotted for the S500 Diesel Oil pollutant used in numerical simulation based on time and mean temperature.

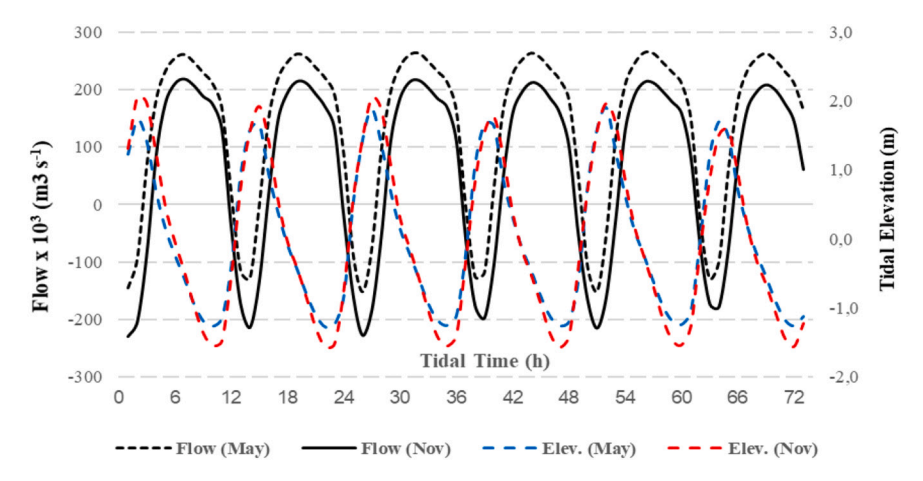


Fig. 4. Variation in the flow (m³ s⁻¹) and elevation of the simulated surface level (m) calibrated by SisBaHia software for May and November. Spill time up to 72 h.

concentration variation in the range from 100% to 50%, on average, in the time interval between 1 and 72 h.

The specific mass of fuel oil used in the numerical simulation model was $\rho_{fuel}=830~kg~m^{-3}.$ The spilled volume was $V=10,416~m^3,$ if one takes into consideration a ship whose tank has 50,000~t of total capacity, subdivided into 12 sub-tanks. The simulation took into consideration that only two of these sub-tanks were damaged and caused the spill. Containment barriers were not taken into consideration in the simulation. Assumingly, the spill started at the end of the flood tide (most likely quadrature tide). For brevity and convenience, the simulation time limit to disperse the selected fuel oil was set at 72~h, at intermediate output intervals of 18,~24,~48 and 72~h. But, in addition, all the complete simulations, carried out at regular intervals every 6~h, are described in detail in the "Supplements" files.

2.4.4. Tidal behavior and hydrodynamic parameters

The tide flow and amplitude curves shown in Fig. 4 were numerically generated in SisBaHia based on the calibrated and validated hydrodynamic model (Abreu et al., 2020). Colors indicate different seasonal periods (May and November). The flow in the dry period (November) and, consequently, the hydraulic energy of the Amazon River significantly decreases in comparison to the flow in the rainy period (May) (Valerio et al., 2018). The hydraulic energy decrease in the summer increases the influence of the Atlantic Ocean on the Amazon River. In addition, it can significantly change among different years, mainly in the dry period or in events such as El Niño or La Niña (Da Cunha and Sternberg, 2018).

Thus, simulations of accidents with fuel oil spills always started 1 h before the maximum tide peak. In other words, the initial fuel oil spill time ($t_0=1\,h$) was used in all reference scenarios (S-1, S-2, S-3 and S-4) and lasted up to 72 h. This maximum time interval was enough to assess the space-time variation of the pollutant plume in all four tested scenarios.

2.4.5. Statistical analysis and model evaluation

Statistical analyses were performed to compare the simulated results of tides generated in the SisBaHiA based on experimentally recorded data or on data recorded at the tide station of Port of Santana, both in May and in November. May and November 2019 were used as reference periods by following the same methodology used by Abreu et al. (2020).

Thus, the following statistical tests were applied to quantify the efficiency of mathematical models: Nash-Sutcliffe (NSE) (Eq. (9)), Person's Correlation, R² and Agreement Index (d) (Eq. (10)). These tests were used due to their different practical applications in hydrodynamic modeling to test models' accuracy and ability to represent the physical reality of natural flows (Baranyi et al., 2002; Mari et al., 2007; Obertegger et al., 2007; Liu et al., 2011; Huang et al., 2011).

$$E_{NS} = 1 - \frac{\sum_{i=1}^{n} (O_i - P_i)^2}{\sum_{i=1}^{n} (O_i - \overline{O})^2}$$
 (9)

$$d = 1 - \frac{\sum |P_i - O_i|^2}{\sum \left(\left| P_i - \overline{O} \right| + \left| O_i - \overline{O} \right| \right)^2}$$
 (10)

Oi and O represent the observed tidal elevations; Pi and P represent values predicted by the model. Model efficiency results can vary between 1 and $-\infty$ in Eq. (2) (Nash-Sutcliffe efficiency), wherein "1" indicates the model capable of perfectly representing the observed data. Values higher than 0.75 indicate that the model is capable of representing experimental observations (Huang et al., 2011). The concordance index test (d) compares data generated by the model (P) to observed data (O): if d=1, the model is considered perfectly coherent; if d=0, the model indicates lack of ability to represent the reality of the observed data set. The minimum value acceptable for "d" is 0.75 (Abreu et al., 2020).

2.4.6. Integrated scenarios between outputs of the hydrodynamic and Lagrangian models and LSI

The integration of numerical simulation methodologies using littoral sensitivity indices (LSI) was defined based on statistical information obtained through AIS data collection. Thus, the risk of accidents can be categorized as the likelihood of having an unwanted event taking place multiplied by the consequences of that same event (Marignani et al., 2017). Moreover, one or more actions could be selected and implemented at the final risk analysis stage to help mitigating these consequences (Xu and Wang, 2014). For example, the degree of risk of accidents can be used based on the potential environmental impacts of the spill, as well as on the operational status of navigation on the waterway. However, littoral sensitivity index (LSI) and its respective local environment must also be taken into consideration (Zanão et al., 2018; Toz et al., 2016; Peixoto et al., 2015; Gurgel et al., 2018; NOAA, 2000).

Thus, the places identified as the most likely to experience accidents comprised four points close to the coastline (≈1 km away from the coast), between Port of Santana in Macapá City and the Curiaú EPA (Figs. 5a-d and 6a-d).

Scenarios indicated in Figs. 5a-d and 6a-d are also relevant because, to the best of our knowledge, they had never been simulated before. In other words, they are essential to help better understanding what would be the most likely periods and places for accidents caused by ships transporting or handling fuel oil on the Lower Amazon River coastline to take place. In addition, it is essential understanding the extent, period and concentration of plumes along the coast of the Lower Amazon River

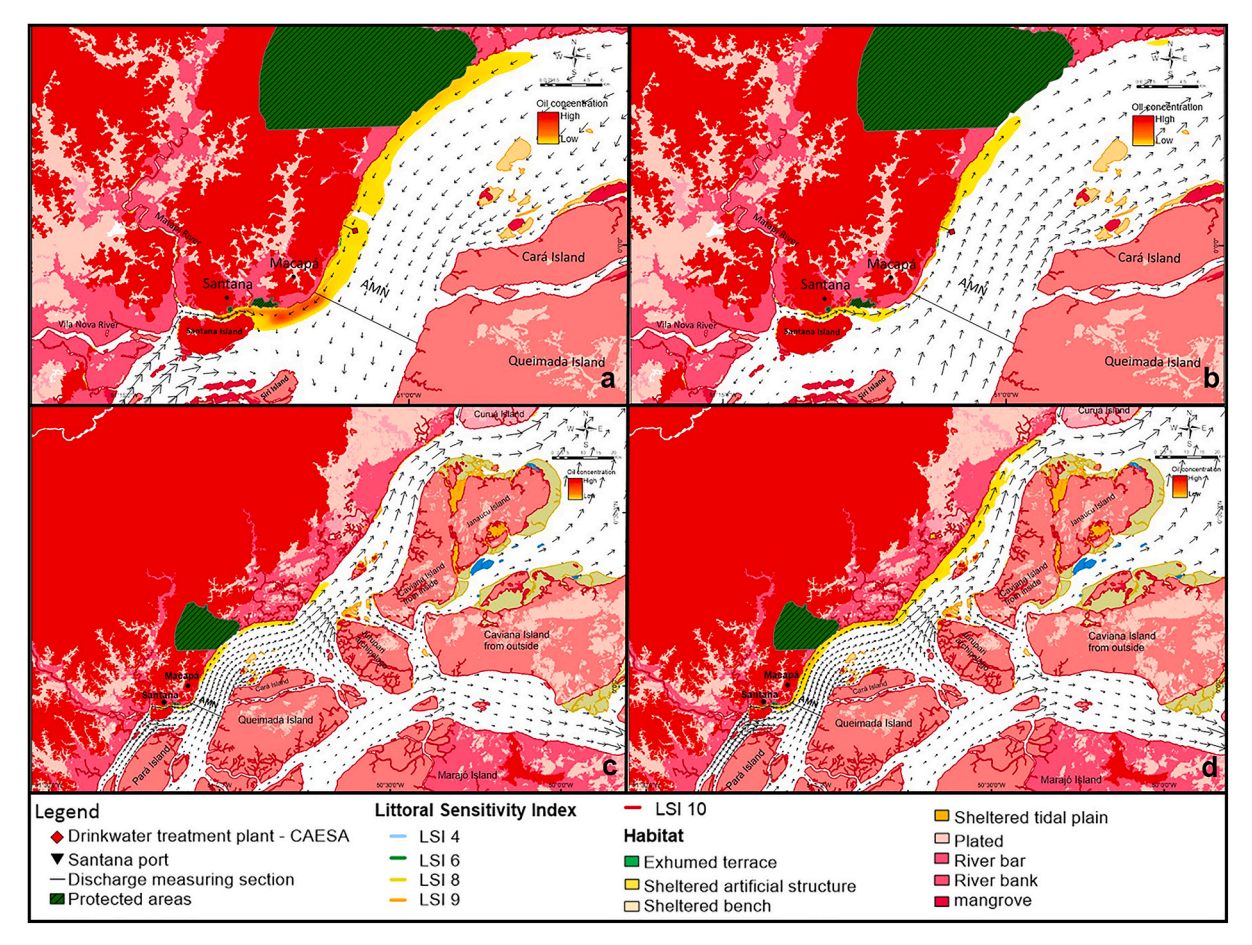


Fig. 5. a-d. Plume dispersion: a) 18 h, b) 24 h, c) 48 h and d) 72 h after the spill started (S-1). May, without significant wind effect.

and areas of interest to protect the biodiversity and human communities that would be most severely affected by oil spills.

3. Results

Only the most critical scenario (S-1) will be presented in this topic due to space limitations in the current article (Figs. 5-d and 6a-d). The remaining scenarios (S-2, S-3 and S-4) were included in supplementary documents. Each scenario presents two different hydrological conditions, namely: rainy (May) and dry (November). The concentration, length (D) and width (W) of the plume and its proximity to the coastline (L) were the criticality parameters used to define the relevance of the scenario.

3.1. Plume dispersion and impact on the coastline and on local biodiversity

Figs. 5 and 6 show the results of the S-1 modeled and simulated scenario. This scenario has simulated an oil spill accident at Companhia Docas do Porto de Santana (DCPS). Plume behavior resulted from its spatial-temporal variation during three semidiurnal tidal cycles, between 1 h and 72 h. This period-of-time was considered adequate to test the limits of the most immediate accident-response conditions.

Figs. 5a-d and 6a-d show the dispersion dynamics of the S500 oil at 18, 24, 48 and 72 h after oil spill in the water (scenarios S-1 of May and November, respectively).

Fig. 5a-d are presented in different spatial scales to allow fully visualizing the extension of plumes. Flow vectors indicate the direction and speed intensity of currents in the Amazon River. It is important noticing that the contact area of the oil plume extends over extremely

sensitive LSI sections (LSI \geq 9.0).

Table 2 presents the results of scenarios (S-1, S-2, S-3 and S-4) with physical and geometric details of the dispersion of polluting plumes. Time intervals t_1 , t_6 , t_{12} , t_{18} , t_{24} , t_{48} and t_{72} h were used to identify different scenarios. It also indicates dispersive features of the plumes for emission sites and simulated scenarios, in comparison to the littoral sensitivity index (LSI), biotic occurrences, as well as to the representation of local habitats and ecosystems and of socioeconomic (urban) resources.

L=0 means that the plume touches the coast. In all four tested scenarios S-1, S-2, S-3 and S-4 (both in May and in November), the plumes touch long extensions of the coast in proportion to the longitudinal distance (D), hydrological period and tide phase. On the other hand, the plume extends for up to $132~\rm km$ and always touches the coast in the rainy season of the S-1 scenario (the most severe scenario). Plume width (W) tends to expand to at most 6 km, on average. However, plumes in scenarios S-3 and S-4 are wider in the dry period (November); they get increasingly larger the further downstream of the Amazon River in comparison to the initial oil spill point (CAESA and Curiaú EPA). The aforementioned plume widening during the rainy season is not so evident in scenarios S-1 and S-2 (Port of Santana, S-1 and Santana Channel, S-2).

For example, in the S-1 scenario, the plume would impact the port zone near Port of Santana, the urban areas of Macapá and Santana cities, Fazendinha and Curiaú EPAs, as well as different aquatic and terrestrial species of the biota identified in the legend of Fig. 7.

LSI, wind effects and ranking of impacts can be qualitatively observed in the last three columns of Table 2. LSI in the S-1 scenario (May and November) is extremely sensitive (LSI \geq 9), whereas in May (rainy), the winds resulted in NE (neutral). However, wind intensity in

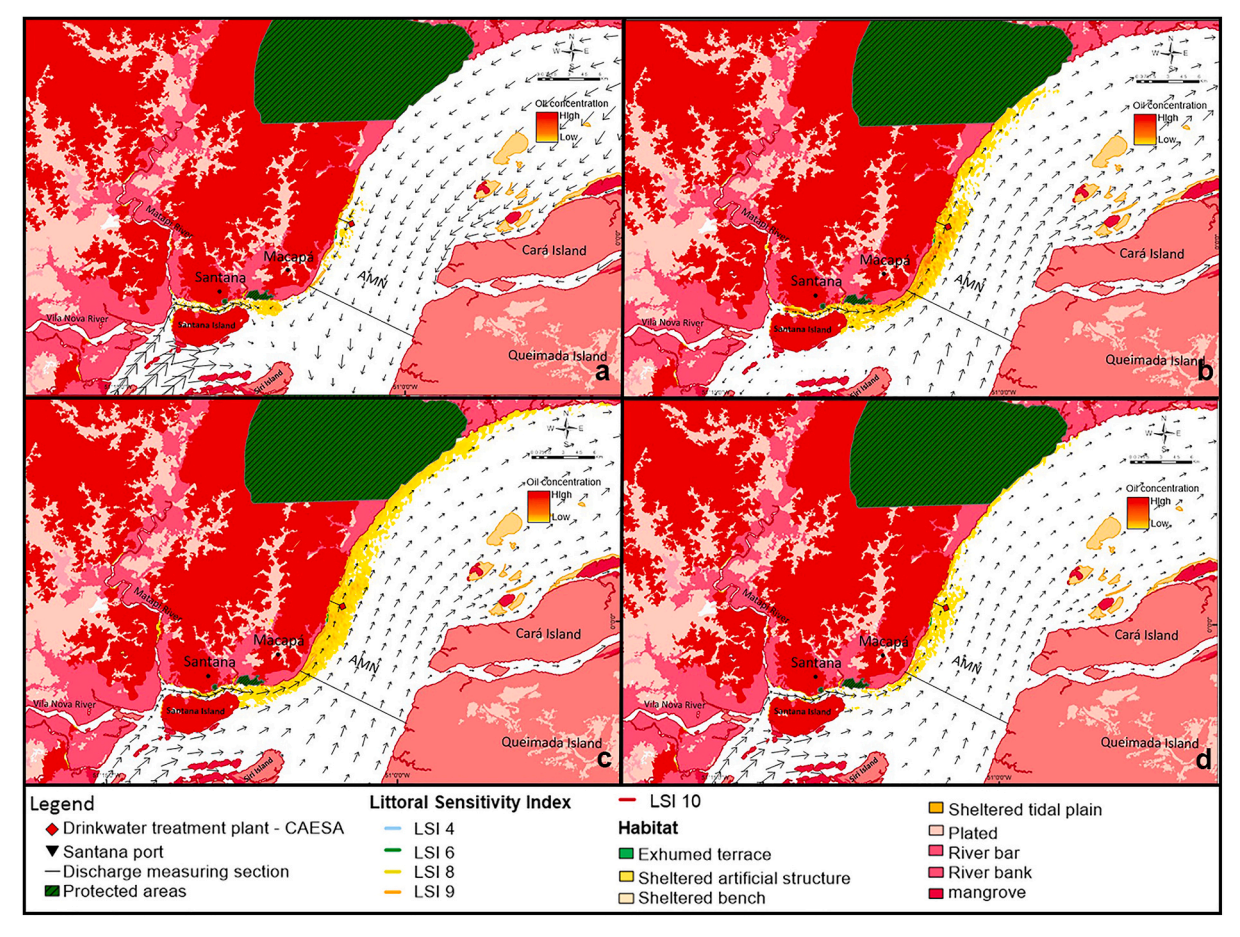


Fig. 6. a-d. Plume dispersion: a) 18 h, b) 24 h, c) 48 h and d) 72 h after the spill started (S-1). November (with significant wind effect).

November (dry season) was NF (not favorable to dispersion), since trade winds intensify from the Amazon River Channel towards the coast - Northeast-Southwest direction) with lesser plume extension (D). Therefore, the plume tends to fragment more in the dry season (November), when there is reduced concentration of the most dispersed oil stains on the coast due to increased temperature, higher evaporation rate, as well as to wind effect, which favors the emergence of waves. In fact, the environmental risks represented in Table 2 by environmental impact types "A" (Environmental Protection Areas), "B" (Water Treatment Station - CAESA) and "C" (Ecological/Biota) could also be qualitatively mapped. For example, according to results in Table 2 and Fig. 7, if there was an oil spill accident similar to that of scenario S-1 (May), it would be necessary to stop the water supply for at least 3 consecutive days, only if the oil spill would definitely stop after 72 h.

Thus, scenarios S-1 and S-2 appear to be more severe in environmental and ecological risks (classes A, B and C) than scenarios S-3 and S-4. This outcome means that the closer the oil spill is to Port of Santana, the more severe the consequences will be. In addition, the impacts on socioeconomic resources and local biodiversity would be significantly stronger.

4. Discussion

The numerical modeling and simulation process has included new priorities and perspectives of contingency plan users in the event of oil spill accidents in the Lower Amazon River. It was possible illustrating four scenarios that can be used as basic reference and applied to support the emergency response, trainings and safety planning.

All four simulated scenarios provide unprecedented support to emergency response priorities by detecting the sensitivity of the coastal

area and supporting decision makers. Based on data about the impacted area and the time the plume remains in it, it is possible indicating the most reasonable method to help mitigating and controlling spills, as well as taking into consideration likely cleaning alternatives (Rodríguez et al., 2007; Shi et al., 2019; Ghiasyand et al., 2021).

Oil plumes can vary in space and time from 0.3 km to 132 km from the fixed pollutant emission point (within up to 72 h); this factor provides a holistic view on the approximate level of extension and potential intensity of the resulting impacts presented by all four tested scenarios, which would directly affect tropical and socio-environmental biodiversity resources in Macapá (docks and urban area, CAESA Water Treatment Station and Curiaú EPA) and Santana (Port of Santana and Fazendinha EPA) cities.

Protected areas such as Fazendinha EPA, Curiaú EPA and the Private Reserve of Natural Heritage (near Macapá) are the most sensitive pollutant-receiving points (IEPA, 2017; Mancio Filho, 2014; Abreu et al., 2020). These urban protected areas extend up to 10 km along the river coast and reach sections presenting high oil sensitivity indices or LSI \geq 9.

It was possible observing that plumes remain in contact with the entire urban area of Macapá and Santana cities, as well as that they would likely extend downstream towards the Atlantic Ocean and reach the islands of Curuá and Bailique (Fig. 7). Studies conducted with domestic organic pollutants close to Macapá City recorded similar behavior for organic pollutant dispersion (Cunha et al., 2012; Pinheiro et al., 2008).

Table 2Dispersive features of plumes for different emission sites and simulated oil spill accident scenarios (S500). S-1, S-2, S-3 and S-4 indicate the places where accidents are most likely to take place in the dry and rainy seasons.

Site/Month (Spill)		Time after oil spill started (hours)						LSI (*)	Wind Effect (**)	Ranking Risk A, B, C (***)	
Site	Month	1	6	12	18	24	48	72			
Physical features of the plume (km)											
S-1 (Port of Santana) (Present Study)	May	W:0.3 L:0.06 D:2	W:1.4 L:0 D:14	W:1.1 L:0 D:10	W:2.6 L:0.0 D:44	W:1.9 L:0 D:48	W:2.3 L: 0.0 D: 75	W:3.5 L:0.0 D:132	9	NE	A,B,C
	November	W:0.3 D:0.06 C:2.8	W:1.4 L:0 D:9.5	W:2.1 L:0 D:25	W:1.5 L:0 D:26	W:1.8 L:0 D:37	W:2.4 L:0 D:55	W:2.3 L:0 D:55	10	NF	A,B,C
S-2 (Santana Channel) (Supplementary File)	May	W:0.2 L:0.6 C:1.8	W:2 L:0 D:15	W:1.3 L:0 D:31	W:2.4 L:0 D:40	W:1.3 L:0 D: 50	W:1.3 L:0 D:54	W:3.1 L:0 D:75	9	NE	A,B,C
	November	W:0.3 L:0.6 C:2.6	W:1.7 L:0 D:12	W:1.3 L:0 D:27	W:2.2 L:0 D:30	W:1.8 L:0 D:36	W:1.7 L:0 D:50	W:2.0 L:0 D:70	10	F	A,B,C
S-3 (Pedrinhas River) (Supplementary File)	May	W:0.27 L:3.7 D:1.8	W:1.8 L:2.5 D: 19	W:3.2 L:1.3 D:32	W:4.7 L:0.9 D:50	W:3.4 L:0.6 D:33	W:5.7 L:0.5 D:74	W:5.7 L:0 D:122	9	NE	В,С
	November	W:0.30 L:3.7 D:3.7	W:1.5 L:2.1 D:14	W:2.7 L:1.8 D:26	W:2.4 L:1.0 D:31.5	W:3.3 L:1.5 D:38	W:2.7 L:0.5 D:50	W:6.1 L:0 D:72	9	F	В,С
S-4 (CAESA) (Supplementary File)	May	W:0.25 L:2.5 D:2.8	W:1.3 L:1.2 D:18	W:1.3 L:0.75 D:35	W:4.1 L:0.0 D: 50	W:1.8 L:0.0 D:35	W:5 L:0.0 D: 75	W:5.0 L:0.0 D: 120	10	NE	В,С
	November	W:0.5 L:2.5 D: 5	W:1.5 L:1.4 D:13.9	W:2.4 L:0.6 D:29	W:1.9 L:0 D:37	W:2.4 L:0 D:40.5	W:3.6 L:0 D:50	W:6.8 L:0 D:71	9	F	В,С

W = Plume width (maximum value, km); D: Plume length (extension of the oil spill point, km); L: Minimum distance from the coast (or coastline, km).

Notations and Symbology

- (***) Typology of Environmental Impact A (Environmental Protection Areas), B (Water Treatment Station CAESA), C (Ecologically/Biota).
- (**) Wind effect (F = Favorable to dispersion on the coast, NF = Not favorable to dispersion on the coast, and NE = No Effect or Neutral).
- (*) Littoral Sensitivity Index (ISL ESI Charts) = 1, 2, 3, 4, 5, 6, 7, 8, 9 and 10 (IEPA, 2017). Scenarios highlighted in gray represent the most disadvantaged situation. In other words, the greater the expansion of the plume, the greater the environmental impact on the coastline.

4.1. Environmental scenarios of S500 oil plume dispersion behavior in the coastline

Although accidents in inland waters are less frequent than oceanic accidents, several regions worldwide are susceptible to impacts directly caused by petroleum products. According to IEPA (2017), 84% of Amazonas River Mouth coastline presents maximum LSI, i.e., LSI = 10. Therefore, this coastline is extremely sensitive to oil spills and requires constant planning and risk monitoring (Araújo et al., 2014; EPBR, 2020).

The impact of crude oil or other similar pollutants on the environment depends on specific features of these pollutants and on the influence of the affected environment (temperature, oil type, current conditions, tide, wind). For example, hydrodynamics plays extremely relevant role in several biogeochemical, hydrological or operational scenarios (S-1, S-2, S-3 and S-4) that influence pollutant dispersion processes (Abreu et al., 2020), organic matter (Ward et al., 2013; Ward et al., 2016) and sediment transport (Santos et al., 2018; Torres et al., 2018), lateral connectivity with the main rivers and lake areas on the coast (Da Cunha and Sternberg, 2018), as well as seed dispersion and genetic flow (Da Cunha et al., 2017).

It is worth highlighting that tidal influence in November (lesser rainy period) intensifies the inversion of the flow in the Amazon River (Abreu et al., 2020). This factor competes with river breeze effect and intensification processes, which enable longer plume permanence close to the coast, but also intensify evaporation effects due to temperature increase (Da Cunha and Sternberg, 2018).

These effects were observed in all four tested scenarios, where plumes tended to breakdown in the dry period (November). Thus, plumes remained in a more restricted and impacted section, which was not observed for the rainy season (May). In addition, they tended to lose their continuous appearance in all dry period scenarios. In this case, two factors controlled the dispersive processes during both seasonal periods, namely: the hydrodynamic influence of the dry period and the sensitive influence of temperature and wind, which acted on the chemical kinetics of the reaction and on the evaporation rates (stronger breeze) (Kuhn et al., 2010; Da Cunha and Sternberg, 2018).

Light oils such as S500 are also more easily absorbed by the biota, since they act at cellular level and have immediate toxic effect on plants (Lopes et al., 2009). On the other hand, heavy oils cover plants, which leads to asphyxiation and hinders gas exchange (Pezeshki et al., 2000). Oil spills in terrestrial environments directly affect the ecosystem due to soil contamination. On the other hand, the oil floating on the surface of the water in aquatic environments is dispersed by the action of wind and waves in the coastal region. Consequently, it affects terrestrial environments and their vegetation (Pezeshki et al., 2000). In the case of the Amazon region, this dispersion process can be maximized by water level fluctuation due to flood pulse (Junk et al., 1989) and to the effect of estuarine tides on plume dispersion (Abreu et al., 2020; Less et al., 2018).

Thus, eventual oil spills can have immediate effect on the environment, such as generalized death of animals and consequent ecosystem losses. They also have more persistent effects, such as changing animals' behavior and the permanence of oil-derived compounds in the food

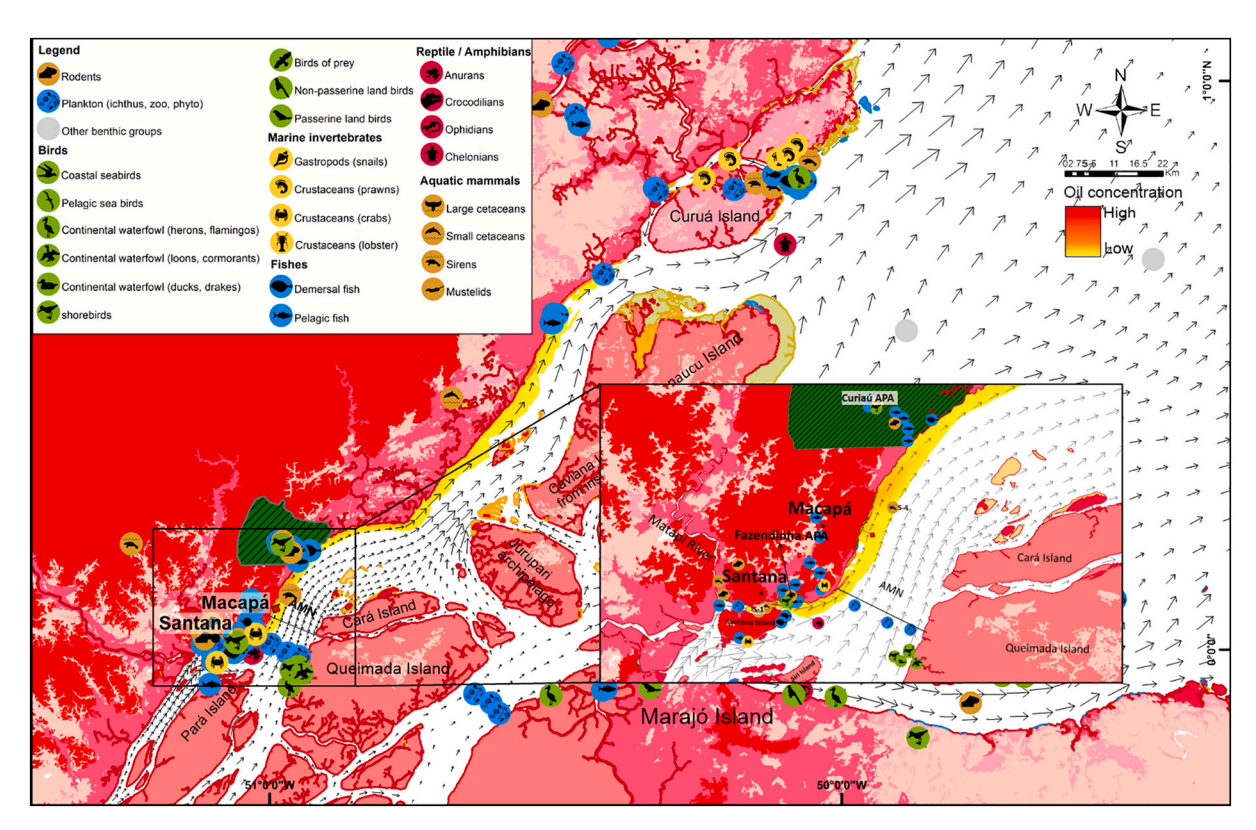


Fig. 7. Scenario S-1 (May) is more impactful when it is integrated to LSI. The dispersion of the simulated plume affects protected areas (in green), the fauna of the tropical biodiversity and human communities (Macapá and Santana cities). Source: adapted from IEPA (2016). (For interpretation of the references to colour in this figure legend, the reader is referred to the web version of this article.)

chain. For example, the broader and continuing perception about habitat and environmental health can be assessed based on the status of indicator species found within these habitats (incidence, distribution and threats to the main habitats and associated indicator species) in order to update the assessment of the local biodiversity state. This critical assessment of data is essential to provide information about the focus of future monitoring and conservation efforts to get environmental policy commitment and a solid foundation for comprehensive ecosystem management projects and strategies (Edmonds et al., 2021).

The potential impacts of oil spills on tropical biodiversity would be concentrated along the length of oil plumes in the Lower Amazon River, which would be in direct contact with plumes along the coast. For example, phytoplankton are the main primary producer of nutrients and oxygen in aquatic environments and play crucial role in primary energy flow into the freshwater food chain (Cunha et al., 2019). For example, algal species *O. croasdaleae* is unable to adapt to the presence of crude oil, and it suggests that oil spills may pose potential risk to the aquatic food chain in benthic zones. Oil can also penetrate the plumage structure of birds, which leads to reduced insulating capacity, makes birds more vulnerable to temperature fluctuations and hinders their ability to fluctuate in water (Oberholster et al., 2014).

The spill of oil or its derivatives in the Lower Amazon River section would certainly compromise the main plant and faunal species population living in these flooded plains (Fig. 7). Thus, it is essential conducting short-term investigations about the potential effects and control of oil spills to help biodiversity conservation areas and the sustainable management of these environments (Lopes et al., 2009).

Thus, oil spills mainly depend on the emission source site, on hydrological period (hydrodynamics), as well as on the wind and traffic of ships that maintain significant part of their trade, including the transport of oil and oil products (Fragoso-Neto et al., 2018; Pereira et al., 2014). Fishing, forestry, biodiversity conservation (Protected Areas) (Dias et al., 2016), tourism and urban water supply systems in Macapá and

Santana cities (Abreu et al., 2020) are the activities mostly threatened by oil spills.

Although some spilled oil separation technologies have emerged such as the use of polystyrene nanofibers, which are highly effective in removing different spilled oil types and, therefore, can be used as inexpensive, available, reusable, ecological technology to efficiently remove oil pollution from the water (Ghiasvand et al., 2021) - they were never applied in Amazonian estuarine environments.

4.2. Simulation of S500 oil plume spillway on the coastline (scenario 1 = S-1, May and November)

Oil spill modeling procedures have been often investigated in the literature. Vairo et al. (2016) have used the MIKE (3D) model to model the dispersion of oil spilled by ships. Hypothetically, the oil spilled in a given port area would be trapped in recirculation in the first 4 h and affect several regions close to the hypothetical accident site. In these cases, the aforementioned authors have suggested hydrodynamic complexity in association with wind effects that would influence the behavior of coastal currents and dispersive processes, such as recirculations around the analyzed key areas. According to them, a model integrated with experimental data enables estimating the global risk of oil spills with reasonable and appropriate results. Thus, they have suggested that the knowledge generated from this approach could help minimizing future coastal environmental impacts on sensitive areas, as well as supporting responses to local oil spills.

Palazzi et al. (2004) have also used mathematical models of different complexities in dispersion studies conducted after oil spill in the open sea. Different phenomena involved in the evolution of the spill were quantified, namely: convective transport by sea currents; wave action; turbulent diffusion; floating action on dispersed particles; superficial oil spreading due to different sea water and hydrocarbon densities; as well as evaporation and emulsification rates. Besides the environmental

consequences, the most severe hazards resulting from leaks in the port area are linked to fires and explosions caused by flammable clouds formed by evaporated hydrocarbons/air mix, as well as to subsequent ignition in the event of accidents. However, the aforementioned study took into consideration explosions taking place in confined areas and focused on analyzing the individual intervention time and the most appropriate approaches to keep the risk at acceptable level - the intervention and dispersion times must be comparable. Thus, according to Palazzi et al. (2004), the basic variables used to develop their mathematical model comprised oil spill dispersion rate, hydrocarbon evaporation rate, pollutant plume transport in water and dispersion in the atmosphere, which were the most relevant parameters. Although the model was simplified, it allowed identifying risk areas and times of intervention in confined regions and ports.

Issues caused by accidents in the open sea or in estuarine or port areas are quite different, mainly when large oil volume is released in the environment in a short period-of-time. However, most protective actions observed in the literature, such as measures to contain and recover spilled oil, are mainly based on the knowledge about the longer-term phenomenon evolution (Palazzi et al., 2004).

The present study has shown how a numerical model can be applied to intervention time actions and to actions taken to mitigate the impact caused by oil spills. Results shown in Figs. 5a-d, 6a-d, 7 and in Table 2 (supplementary file) suggest that the observed risks only provide basic, although crucial, information to support the adequate assessment of eventual environmental impacts caused by oil spills in the Lower Amazon River region.

The integration between numerical simulation and LSI data depending on the specific scope of the assessment - is also extremely useful for the analysis of potential impacts caused by oil spills on geomorphologically and biologically sensitive environments (Dias et al., 2016; Santos et al., 2018) that are relatively unknown (IEPA, 2017). In addition, likely oil spills could severely affect urban areas of high socioeconomic interest. Therefore, similar numerical studies can be used as subsidy to support and plan ecological protection actions focused on potentially impacted socioeconomic resources (IEPA, 2016; Mancio Filho, 2014).

Numerical analyses integrated with LSI can be used to complete or subsidize management and conservation plans developed at basin scale, as well as environmental impact assessments at local scale. As simulations often take into account multiple potential sources and different release times to analyze the variability in response times and danger on the coast due to variability in atmospheric and fluvial conditions, it is necessary using the probability of these scenarios to estimate plume dispersion in order to support eventual tactical/operational demands (Melaku Canu et al., 2015).

It is essential integrating environmental sensitivity (LSI) with modeling and numerical simulation to help better understanding the likely dynamics of plumes and to protect coastal areas from accidental or illegal spills. On the other hand, this integration is a crucial element to acknowledge the work of Operational Agencies in case of potential crisis (Sayol et al., 2014), at the following operational sequence: i) the exact position of the accident at the early stages of a real crisis is often unknown, and it generates inaccurate initial conditions in the predictive model; ii) the dispersion of a plume in the flow depends on the area exposed to the wind and on its angle of attack; iii) these influences are often included in the wind drag coefficient (Sayol et al., 2014). For example, based on these very same reasons, plumes obtained by numerical simulation in the S-1 scenario (May and November) were significantly different from each other, mainly at longer time intervals, between 18 and 72 h (Table 2). Consequently, there was greater plume fragmentation in the dry season (November) due to greater effect of fluvial winds, higher temperatures and likely intensification of evaporation processes (Kuhn et al., 2010).

4.3. Integration between S500 oil plume spillway simulation and LSI in the shoreline

Coastal classifications depend on the physical substrate of the coast, which determines pollutants' persistence in it, based on materials' capacity to retain them. Thus, the following criteria are often used for such a classification (Sayol et al., 2014): a) coastal elevation also determines accessibility to perform cleaning and restoration tasks in case of contamination events; b) degree of exposure to wave energy: there are mainly two coast types when it comes to the influence of waves. The first type corresponds to coasts exposed to waves (high-energy coasts), where pollutants tend to be naturally and more easily removed. The second type corresponds to protected coasts (low-energy environments) where the spill is gradually removed; c) degree of exposure to wave energy is determined by the coast articulation degree (cables, natural harbor, bays, inlets), as well as by bathymetry, which conditions the wave energy dissipation and allows wave "trains" to reach the coast; d) substrate type: the most important distinction lies between rocks and unconsolidated sediments. Penetration depth is controlled by substrate grain size and can lead to long-term biological impacts (IEPA, 2017); and e) biological sensitivity, which refers to the ability of the coastal environment to shelter different habitat types (Lopes et al., 2009).

According to the present simulation analysis, the coastal types of the Lower Amazon River are relatively unfavorable to ecological recovery after eventual oil spills, mainly because they are closely related to fragile geomorphology (Torres et al., 2018), intense hydrodynamic and hydrological processes (Abreu et al., 2020) and, mainly, to biodiversity fragility along the coast (Dias et al., 2016).

The integration between LSI information and information about the dispersion of oil or oil-derivative plumes based on numerical modeling, and the likelihood of oil spill accident capable of affecting a given environment, can be used to generate environmental vulnerability maps in order to rapidly and easily indicate the areas that should receive priority protection after spills. In addition, the LSI planning tool integrated with numerical oil dispersion simulations can be extremely useful to map eventual cleaning procedures and response actions. It also allows fast impact visualization and decision making by those accountable for taking emergency actions (Romero et al., 2014). In addition, international recommendations often mention maps of environmental vulnerability to oil, which should be drawn after taking into consideration the likelihood of having the oil reaching a certain area.

Although there have never been accidents with ships and oil spills at large proportions, there is the permanent threat and risk of accidents in the Lower Amazon River region due to the traffic of ships carrying oil or derivatives, mainly with ships sailing at speed faster than 10 knots. Moreover, exploration projects implemented at the Amazon River mouth have faced strong resistance from environmentalists and great demand for data and information by Ibama (Brazilian Institute of Environment and Renewable Natural Resources). Licensing is often followed by environmental preservation organizations, after the discovery of an offshore oil exploration area (at least 9.5 $\rm km^2)$ dominated by rare coral reef capable of surviving in the murky waters of the Amazon region (EPBR, 2020).

4.4. On oil spill contingency plans

Despite the risks observed in the study site, oil spill contingency plans (OSCPs) remain unavailable. However, according to Shi et al. (2019), it is extremely relevant evaluating the feasibility of oil spill contingency plans (OSCPs) in a systematic manner, based on the information availability and accuracy perspective. Therefore, conceptual models focused on integrating fundamental elements of contingency plans must be available, as well as relevant information flows to enable emergency response to eventual oil spills. The aforementioned author adopted the Dempster-Shafer (D—S) approach to develop a series of models to assess the feasibility of contingency plans related to the

managerial information to mitigate environmental impacts. The models were validated through a case study, which concluded that simplifying information requirements and improving the availability and accuracy of key information are effective methods used to improve the informative feasibility of contingency plans.

An example of information lies on GIS (LSI) using to assess the estimated risk of oil spills, as described by Milazzo et al. (2010), who applied quantitative analysis to the risk observed in overland transport of hazardous materials in Sicily - Italy. The risk was calculated based on the TRAT-GIS code, which is a software used to assess incidental and environmental risks associated with the transport of dangerous substances and supported by the Geographic Information System (GIS). Results were inserted in a database and the GIS allowed displaying the risk maps. Although this analogy is based on overland transport, comparisons between different transport types and routes have been performed through risk maps in order to reduce these risks and to better protect biotic and socioeconomic resources.

The modern traffic trend of large cruise ships, which can also pose a serious threat in terms of passengers' evacuation/rescue and potential impact on likely environmental targets is an interesting aspect of this analysis type. Vairo et al. (2016) have critically analyzed three accidents involving passenger ships. They have assessed the risk, acceptance criteria and sea-use planning in association with cruise activity in the worldwide known sensitive area of Portofino (Italy). In order to do so, they adopted a numerical method approach, similar to the one used in the present study, to evaluate consequences and effects, dangerous distance and reaction time scale associated with fuel spills and smoke-spreading fire scenarios.

According to the aforementioned authors, the numerical approach can be a powerful tool to design ideal navigation routes and temporary mooring points by balancing economic issues and mitigating the physical impact on sensitive biological communities. This approach suggests that risk studies about vulnerable coastlines play essential role in the preparation for oil spills and can be carried out based on the assessment of ship traffic and of the likelihood of accidents in, and impacts on, neighboring waters. Thus, it is possible providing technical basis for emergency planning, based on adequate response equipment and, consequently, minimizing the impact of spills on the coast. Therefore, even accidents with passenger ships can release oil in water, which is the reason why they are considered a serious threat to coasts and marine/estuarine environments, with immediate and potential long-term consequences (Vairo et al., 2016).

According to Ellis (2011), accidents also happen with cargo and release of dangerous goods, either packed or in containers, during transport - the consequences of these accidents on board a ship can be severe. The aforementioned author has identified contributing factors to these types of release, as well as investigated the contribution of accidents with dangerous goods to the overall rates of accident with container ships. Thus, he concluded that most releases - estimated at 97% of events in the USA and 94% of events in the United Kingdom - did not happen after primary accidents, such as collisions; they took place due to the incidence of failures during activities such as preparing the goods for transportation, packaging, container filling and loading.

5. Conclusions

The herein presented methodology enabled making a comprehensive and consistent first-order assessment of the qualitative risk of oil spills in coastal areas along a section representative of the Lower Amazon River.

The urban areas of Macapá and Santana cities, as well as a wide range of nearby coastal ecosystems, may be threatened by eventual oil spill accidents, whose potential environmental impacts require taking intelligent and rigorous planning measures, in addition to contingency, inspection, monitoring and ship control actions. The area potentially affected after only 72-h oil spill would require significant operational effort that, apparently, is not available in the region. In other words,

there are no technical studies, teams and equipment currently available to deal with accidents similar to the ones proposed in scenarios S-1, S-2, S-3 and S-4.

Communities of several coastal aquatic biota species, as well as the coastal zone closest to Macapá and Santana cities, are the most vulnerable places in case of fuel oil spill caused by ship accident. Based on the analyzed scenarios, the rainy hydrological period, during the low tide, is the most critical time because it is when the most persistent and intense plume dispersion process takes place. With respect to the dry hydrological period (November), although plumes are shorter in length, they get wider within a 72 h dispersion period due to stronger wind effect and flood in this period.

With respect to the maximum qualitative risk assessment of polluting plume accidents, the greatest potential for coastal water contamination (urban areas, drinking water treatment plant, ecosystems) would also be observed in the rainy season (May), during the low tide. Thus, the maximum extent of oil-deriving pollutant plumes would be observed at the distance of up to 132 km along the left bank of the Amazon River within only 72 h.

This outcome confirms the hypothesis that plumes tend to disperse close to sensitive coastlines [LSI ≥ 9.0] and over long distances, a fact that compromises cities, riverside communities, local fauna and flora, if one takes into consideration the critical points and plume emission time intervals, as well as the likelihood of accidents described for ships traveling in the region identified by AIS.

Although the present results are at initial stage, operational ISE charts were tested for the first time in the investigated Lower Amazon River section. To the best of our knowledge, there is no information available in the literature about the qualitative and quantitative monitoring of oil spills in this region.

Finally, further field and experimental studies should be conducted in other sections of the Lower Amazon River estuary, in order to transcend the port area and the main large-scale navigation waterway of the Lower Amazon River and, therefore, to enable solving and detailing oil spill issues at operational level in order to stop them, as well as their potential environmental impacts.

CRediT authorship contribution statement

Alan Cavalcanti da Cunha: Conceptualization, Methodology, Formal analysis, Investigation, Resources, Data curation, Writing – original draft, Writing – review & editing, Visualization, Supervision, Project administration, Funding acquisition. Carlos Henrique Medeiros de Abreu: Methodology, Software, Validation, Formal analysis, Investigation, Data curation, Writing – original draft, Writing – review & editing, Visualization. Jonathan Luz Pires Crizanto: Methodology, Software, Validation, Formal analysis, Investigation, Resources, Data curation, Visualization. Helenilza Ferreira Albuquerque Cunha: Formal analysis, Investigation, Writing – original draft, Writing – review & editing, Visualization, Supervision. Alaan Ubaiara Brito: Formal analysis, Investigation, Writing – original draft. Newton Narciso Pereira: Methodology, Formal analysis, Investigation, Data curation, Writing – original draft, Writing – review & editing, Visualization, Supervision.

Declaration of competing interest

None

Acknowledgment

The authors are grateful to the Laboratory of Chemistry, Sanitation and Environmental Systems Modeling (LQSMSA), as well as to the National Council of Scientific and Technological Development (CNPq grant: 309684/2018-8), FAPESP grant: 08/58089-9, and NSF DEB Grant: 791 #1256724) for the support. The authors would also like to

thank DPg/PROPESPg/UNIFAP and FUNASA (TR-2018).

Appendix A. Supplementary data

Supplementary data to this article can be found online at https://doi.org/10.1016/j.marpolbul.2021.112404.

References

- Abreu, C.H.M., Brito, D.C., Barros, M.L.C., Teixeira, M.R., Cunha, A.C., 2020.

 Hydrodynamic modeling and simulation of water residence time in the estuary of the Lower Amazon River. Water 12, 1–30. https://doi.org/10.3390/w12030660.
- de Andrade, M.M.N., Souza-Filho, P.W.M.E., Szlafsztein, C.F., 2018. Sensibilidade Ambiental a Derramamento de Óleo e Mapeamento de Unidades de Paisagem na Região Portuária do Maranhão. Revista de Gestão Costeira Integrada. Associação Portuguesa dos Recursos Hídricos (APRH) 18, 73–84. https://doi.org/10.5894/rgcin65.
- Araújo, C.S.T., Hoshina, M.M., Silva, M.T.P., Roberto, M.M., Hara, R.V., Marin-Morales, M.A., 2014. Oil spills: environmental consequences and recovery strategies.
 In: Clifton, A. (Ed.), Environmental Health Physical, Chemical and Biological Factors
 Oil Spills Environmental Issues, Prevention and Ecological Impacts, vol. 4. Nova Science Publishers, New York, pp. 87–120.
- Baranyi, C., Hein, T., Holarek, C., Keckeis, S., Schiemer, F., 2002. Zooplankton biomass and community structure in a Danube River floodplain system: effects of hydrology. Freshw. Biol. 47 (3), 473–482. https://doi.org/10.1046/j.1365-2427.2002.00822.x.
- Calle, M.A.G., Alves, M., 2011. Ship collision: a brief survey. In: Proceedings of COBEM. 21st Brazilian Congress of Mechanical Engineering. Natal, RN, Brazil. http://www.abcm.org.br/app/webroot/anais/cobem/2011/PDF/123201.pdf.
- Cunha, C.L.N., Rosman, P.C.C., Ferreira, A.P., Monteiro, T.C.N., 2006. Hydrodynamics and water quality models applied to Sepetiba Bay. Cont. Shelf Res. 26, 1940–1953. https://doi.org/10.1016/j.csr.2006.06.010.
- Cunha, A. C.; Brito, D. C; Brasil Junior, A. C.; Pinheiro, L. A. R.; Cunha, H. F. A.; Krusche, A. V., 2012. Challenges and solutions for hydrodynamic and water quality in rivers in the Amazon Basin. In: H. E. Schulz et al. (Orgs.). Hydrodinamics: Natural Water Bodies. Book3. Rijeka. InTech Croacia, 3, 67–88. doi:https://doi.org/10.5
- Cunha, E.D.S., Castelo-Branco, R., Silva, L., Silva, N.B., Azevedo, J., Vasconcelos, V., Faustino, S.M.M., Cunha, A.C., 2019. First detection of microcystin-LR in the Amazon River at the drinking water treatment Plant of the Municipality of Macapá, Brazil. Toxins 11, 669–681. https://doi.org/10.3390/toxins11110669.
- Da Cunha, A.C., Sternberg, L.S.L., 2018. Using stable isotopes 18O and 2H of lake water and biogeochemical analysis to identify factors affecting water quality in four estuarine Amazonian shallow lakes. Hydrol. Process. 32, 1188–1201. https://doi. org/10.1002/hyp.11462.
- Da Cunha, A.C., Mustin, K., Dos Santos, E.S., Dos Santos, E.W.G., Guedes, M.C., Cunha, H.F.A., Rosman, P.C.C., Sternberg, L.S.L., 2017. Hydrodynamics and seed dispersal in the lower Amazon. Freshw. Biol. 62, 1721–1729. https://doi.org/ 10.1111/fwb.12982.
- De Souza, E.B., Da Silva Ferreira, D.B., Guimarães, J.T.F., Dos Santos Franco, V., De Azevedo, F.T.M., De Moraes, B.C., 2017. Padrões climatológicos e tendências da precipitação nos regimes chuvoso e seco da Amazônia oriental. Rev. Bras. de Climatol. 21, 81–93. https://doi.org/10.5380/abclima.v21i0.41232.
- Dias, T.C.A.C., Cunha, A.C., Silva, J.M.C., 2016. Return on investment of the ecological infrastructure in a new forest frontier in Brazilian Amazonia. Biol. Conserv. 194, 184–193. https://doi.org/10.1016/j.biocon.2015.12.016.
- EBC (Empresa Brasileira de Comunicação), 2017. http://agenciabrasil.ebc.com.br/geral/noticia/2017-08/acidentes-com-embarcacoes-no-brasil-aumentam-1263-em-2017.
- Edmonds, N.J., Al-Zaidan, A.S., Al-Sabah, A.A., Le Quesne, W.F.F., Devlin, M.J., Davison, P.I., Lyions, B.P., 2021. Kuwait's marine biodiversity: qualitative assessment of indicators habitats and species. Mar. Pollut. Bull. 163, 111915. https://doi.org/10.1016/j.marpolbul.2020.111915.
- Ellis, J., 2011. Analysis of accidents and incidents occurring during transport of packaged dangerous goods by sea. Saf. Sci. 49, 1231–1237. https://doi.org/10.1016/j. ssci.2011.04.004.
- EPBR, 2020. Total reinicia licenciamento ambiental para sete poços na Foz do Amazonas. Mercado offshore. https://epbr.com.br/total-reinicia-licenciamento-ambiental-para-sete-pocos-na-foz-do-amazonas/.
- Fragoso-Neto, J., Pereira, N.N., Cunha, A.C., 2018. Monitoramento da qualidade da água de lastro como suporte à gestão no porto de Santana-AP, Amazônia Estuarina/Brasil. In: Pereira, N. N. (Org.). Água de Lastro Gestão e Controle. 1a ed. São Paulo: Blucher 1, 171–197. https://doi.org/10.5151/9788580393064.
- Gallo, M.N., Vinzon, S.B., 2005. Generation of overtides and compound tides in Amazon estuary. Ocean Dyn. 55, 441–448. https://doi.org/10.1007/s10236-005-0003-8.
- Gallo, M.N., Vinzon, S.B., 2015. Estudo numérico do escoamento em planícies de marés do canal Norte (estuário do rio Amazonas). Revista Iberoamericana del Agua 2, 38–50. https://doi.org/10.1016/j.riba.2015.04.002.
- Ghiasvand, S., Rahmani, A., Samadi, M., Asgari, G., Azizian, S., Poormohammadi, A., 2021. Application of polystyrene nanofibers filled with sawdust as separator pads for separation of oil spills. Process Safety and Environmental Protection 146, 161–168. https://doi.org/10.1016/j.psep.2020.08.044.
- Gil-Agudelo, D. L.; Nieto-Bernal, R. A.; Ibarra-Mojica, D. M.; Guevara-Vargas, A. M.; Gundlach, E., 2015. Environmental sensitivity index for oil spills in marine and

- coastal areas in Colombia. Ciencia, Tecnología y Futuro, 6, 17-28. doi:10.29047/01225383 24
- Gurgel, F.O.M.J., Rosman, P.C.C., Dos Santos, M., 2018. Avaliação de derrame de óleo no entorno do Porto do Forno, Município de Arraial do Cabo, Brasil. XXVIII Congreso Latinoamericano de Hidráulica Buenos Aires, Argentina, In. https://www.ina.gob.ar/congreso_hidraulica/Congreso_libro/TC_TEMA_6.pdf.
- Huang, W., Liu, X., Chen, X., Flannery, M.S., 2011. Critical flow for water management in a shallow tidal river based on estuarine residence time. Water Resour. Manag. 25 (10), 2367–2385. https://doi.org/10.1007/s11269-011-9813-2.
- IEPA Instituto de Pesquisas Científicas e Tecnológicas do Estado do Amapá, 2016. Atlas de sensibilidade ambiental ao óleo da Bacia Marítima da Foz do Amazonas. Coord. Santos, V. F. et al. Núcleo de Pesquisas Aquáticas (NUPAq). https://repositorio. museu-goeldi.br/handle/mgoeldi/1205.
- IEPA Instituto de Pesquisas Científicas e Tecnológicas do Estado do Amapá, 2017. Carta operacional de sensibilidade ambiental ao derramamento de óleo bacia foz do Amazonas Baia de Macapá/Orla de Macapá. Carta FZA 100. Núcleo de Informação em Mídia Eletrônica e Publicação Científica/NUID/IEPA. WebMaster: webadmin@ iepa.ap.gov.br. Núcleo de Pesquisas Aquáticas NUPAq.
- Junk, W.J., Bayley, P.B., Sparks, R.E., 1989. The flood pulse concept in river-floodplain systems. In: Dodge, D.P. (Ed.), Proceedings of the International Large River Symposium. Canadian Special Publication of Fisheries Aquatic Sciences, Ottawa, pp. 110–127.
- Köppen, W., 2020. Das geographische System der Klimate. In: Handbuch der Klimatologie, Köppen W.; Geiger R. Eds. Gerbrüder Borntraeger: Berlin, Germany, 1936(1), 44.
- Kuhn, P. A. F.; Cunha, A. C.; Pereira, M. J.; Saraiva J. B., 2010. Previsão Numérica Operacional no Estado do Amapá Utilizando o BRAMS. In: Cunha, A. C.; Souza, E. B.; Cunha, H. F. A. (Org.). Tempo, Clima e Recursos Hídricos: Resultados do Projeto REMETAP no Estado do Amapá. 1º ed. Macapá - AP: Instituto de Pesquisas Científicas e Tecnológicas do Estado do Amapá - IEPA, 2010, 1, 61-82.
- Less, D.F.S., Cunha, A.C., Sawakuchi, H.O., Neu, V., Valério, A.M., Ward, N.D., Brito, D. C., Diniz, J.E.M., Gagne-Maynard, W., Abreu, C.M., Kampel, M., Krusche, A.V., Richey, J.E., 2018. The role of hydrodynamic and biogeochemistry on CO2 flux and pCO2 at the Amazon River mouth. Biogeosci. Discuss. 1, 1–26.
- Limberger, L.; Silva, M. E. S., 2016. Precipitação na bacia amazônica e sua associação à variabilidade da temperatura da superfície dos Oceanos Pacífico e Atlântico: uma revisão. Geousp Espaço e Tempo 2016, 20, 657–675. doi:10.11606/issn.2179-0892. geousp.2016.105393.
- Liu, W.-C., Chen, W.-B., Hsu, M.-H., 2011. Using a three-dimensional particle-tracking model to estimate the residence time and age of water in a tidal estuary. Comput. Geosci. 37 (8), 1148–1161. https://doi.org/10.1016/j.cageo.2010.07.007.
- Lopes, A., Rosa-Osman, S.M., Piedade, M.T.F., 2009. Effects of Crude Oil on Survival, Morphology, and Anatomy of Two Aquatic Macrophytes from the Amazon Floodplains. https://doi.org/10.1007/s10750-009-9959-6.
 Lu, J., Yuan, V., Mikkelsen, J.D., Ohm, C., Stange, E., Holand, M., 2017. Modelling the
- Lu, J., Yuan, V., Mikkelsen, J.D., Ohm, C., Stange, E., Holand, M., 2017. Modelling the transport of oil after a proposed oil spill accident in Barents Sea and its environmental impact on Alke species. IOP Conf. Ser. Earth Environ. Sci. 82, 012010 https://doi.org/10.1088/1755-1315/82/1/012010.
- Mancio Filho, S. P., 2014. Mapeamento de fontes de poluição por petróleo e derivados e potenciais conflitos com atividades sensíveis ao derramamento de óleo, carta FZA -15, Bacia da Foz do Amazonas. Trabalho de Conclusão de Curso. Curso de Geografia. Universidade Federal do Amapá (UNIFAP). 89p.
- Marengo, J.A., Espinoza, J.C., 2016. Extreme seasonal droughts and floods in Amazonia: causes, trends and impacts. Int. J. Climatol. 36, 1033–1050. https://doi.org/10.1002/joc.4420.
- Mari, X., Rochelle-Newall, E., Torréton, J.-P., Pringault, O., Jouon, A., Migon, C., 2007.
 Water residence time: a regulatory factor of the DOM to POM transfer efficiency.
 Limnol. Oceanogr. 52 (2), 808–819. https://doi.org/10.4319/lo.2007.52.2.0808.
- Marignani, M., Bruschia, D.D., Garcia, D.A., et al., 2017. Identification and prioritization of areas with high environmental risk in Mediterranean coastal areas: a flexible approach. Sci. Total Environ. 590-591, 566–578. https://doi.org/10.1016/j. scitoteny 2017.02.221
- Marinha do Brasil, 2019. Inquéritos Administrativos sobre Acidentes e Fatos da Navegação (IAFNs). https://www.marinha.mil.br/dpc/sites/www.marinha.mil.br. dpc/files/Quadros%20Estat%C3%ADsticos%20ANO%202018%20DADOS%20AT%C3%89%2030%20SET%202019.pdf.
- Marinho, C., 2012. Avaliação do Índice de Sensibilidade do Litoral (ISL) no âmbito das Cartas SAO: Identificação de lacunas e proposição das variáveis biológicas em sua composição. Dissertação de Mestrado. Pós-Graduação em Oceanologia. Universidade Federal do Rio Grande 1, 1–82.
- Melaku Canu, D., Solidoro, C., Bandelj, V., Quattrocchi, G., Sorgente, R., Olita, A., Fazioli, L., Cucco, A., 2015. Assessment of oil slick hazard and risk at vulnerable coastal sites. Mar. Pollut. Bull. 94, 84–95. https://doi.org/10.1016/j.marrollyll/2015.02.006
- Milazzo, M.F., Lisi, R., Maschio, G., Antonioni, G., Spadoni, G., 2010. A study of land transport of dangerous substances in eastern Sicily. J. Loss Prev. Process Ind. 23, 393–403. https://doi.org/10.1016/j.jlp.2010.01.007.
- MMA / SQA (Ministério do Meio Ambiente / Secretaria de Qualidade Ambiental nos Assentamentos Humanos). Especificações e normas técnicas para a elaboração de cartas de sensibilidade ambiental para derramamentos de óleo. Brasília, 2004. 107 p.
- Montewka, J., Hinz, T., Kujala, P., Matusiak, J., 2010. Probability modelling of vessel collisions. Reliability Engineering & System Safety 95, 573–589. https://doi.org/ 10.1016/j.ress.2010.01.009.
- Mou, J.M., Van der Tak, C., Ligteringen, H., 2010. Study on collision avoidance in busy waterways by using. AIS data Ocean Engineering 37 (5), 483–490. https://doi.org/ 10.1016/j.oceaneng.2010.01.012.

- NOAA, 2000. ADIOSTM (Automated Data Inquiry for Oil Spill) version 2.0 Seatle: Hazardous materials Response and Assessment Division, NOAA. Prepared for the U. S. Coast Guard Research and Development Center, Groton Connecticut.
- Oberholster, P., Cheng, P., Truter, C., Hill, L., Botha, A.M., 2014. Species specific responses of common freshwater wetland phytoplankton to crude oil by application of bioassays. Chapter 10, 197-213. In: Clifton, A. (Ed.), Environmental Health Physical, Chemical and Biological Factors Oil Spills Environmental Issues, Prevention and Ecological Impacts. Nova Publishers, New York.
- Obertegger, U., Flaim, G., Braioni, M.G., Sommaruga, R., Corradini, F., Borsato, A., 2007. Water residence time as a driving force of zooplankton structure and succession. Aquat. Sci. 69 (4) https://doi.org/10.1007/s00027-007-0924-z.
- Padovezi, C.D., 2012. Avaliação de riscos do transporte fluvial de passageiros na Região Amazônica. In: In: Congresso nacional de transporte aquaviário, construção naval e offshore, 24. Janeiro. Anais, Rio de (6 p).
- Palazzi, E., Curro, F., Fabiano, B., 2004. Simplified modelling for risk assessment of hydrocarbon spills in port área. Process. Saf. Environ. Prot. 82 (B6), 412–420. https://doi.org/10.1205/psep.82.6.412.53200.
- Pedersen, P.T., 1995. Collision and grounding mechanics. In: The Danish Society of Naval Architects and Marine Engineers, Copenhagen. Proc. WEGEMT, vol. 95, pp. 125–157
- Peixoto, C. G. D.; Costa, Y. L. S.; Araujo, A. S.; Fernandes Junior, V. J., 2015. Caracterização Físico-Química de Óleo Diesel Rodoviário e Marítimo por Técnicas Convencionais e Destilação Simulada por Cromatografia Gasosa. (Apresentação de Trabalho/Congresso).
- Pereira, N.N., 2007. Um estudo sobre instalações propulsoras para empurradores fluviais. Dissertação de mestrado. Universidade de São Paulo 2007.
- Pereira, N.N., Botter, R.C., Folena, R.D., Pereira, J.P.F.N., Da Cunha, A.C., 2014. Ballast water: a threat to the Amazon Basin. Mar. Pollut. Bull. 84, 330–338. https://doi.org/10.1016/j.marpolbul.2014.03.053.
- Pezeshki, S.R., Hester, M.W., Lin, Q., Nyman, J.A., 2000. The effect of oil spill and cleanup on dominant US Gulf coast marsh macrophytes: a review. Environ. Pollut. 180, 129–139. https://doi.org/10.1016/S0269-7491(99)00244-4.
- Pinheiro, L.A.R., Cunha, A.C., Cunha, H.F.A., Brito, D.C., Saraiva, J.B., 2008. Aplicação de simulação computacional à dispersão de poluentes no baixo Rio Amazonas: potenciais riscos à captação de água na orla de Macapá-AP. Amazônia (Banco da Amazônia) 4, 27–44.
- Rodríguez, H., Quarantelli, E.L., Dynes, R.R., 2007. Handbook of Disaster. Springer, Newark, USA. http://nuir.nkumbauniversity.ac.ug/xmlui/bitstream/handle/20.500.12383/1215/Handbook%20of%20Disaster%20Research%20(%20PbFprive%20).pdf?sequence=1.
- Romero, A.F., Fontes, R.F.C., Oliveira, M., Abessa, D.M.S., 2014. New approaches in oil spill mapping and emergency planning. In: Clifton, A. (Ed.), Environmental Health -Physical, Chemical and Biological Factors Oil Spills Environmental Issues, Prevention and Ecological Impacts, vol. 5. Nova Science Publishers, New York, pp. 121–142.
- Rosman, P.C.C., 2018. Referência Técnica do Sisbahia Sistema Base de Hidrodinâmica Ambiental. Engenharia Costeira e Oceanográfica, Rio de Janeiro, Brasil, COPPE. http://www.sisbahia.coppe.ufrj.br/SisBAHIA_RefTec_V10d.pdf.
- Santos, M.G.F., 2013. Análise de acidentes com embarcações em águas sob jurisdição brasileira-uma abordagem preventiva. Dissertação de Mestrado. Universidade Federal do Rio de Janeiro.
- Santos, E.S., Lopes, P.P.P., Pereira, H.H.S., Nascimento, O.O., Rennie, C.D., Sternberg, L. S.L.O., Cunha, A.C., 2018. The impact of channel capture on estuarine hydromorphodynamics and water quality in the Amazon delta. Sci. Total Environ. 624, 887–899. https://doi.org/10.1016/j.scitotenv.2017.12.211.
- Sayol, J.M., Balaguer, P., Conti, D., Rietz, A., García-Sotillo, G., Simarro, G., Tintoré, J., Orfila, A., 2014. Towards an integrated oil spill system: from modelling to the decision support tool. In: Clifton, A. (Ed.), Environmental Health - Physical,

- Chemical and Biological Factors Oil Spills Environmental Issues, Prevention and Ecological Impacts, vol. 3. Nova Science Publishers, New York, pp. 67–86.
- Shi, X., Wanga, Y., Luob, M., Zhang, C., 2019. Assessing the feasibility of marine oil spill contingency plans from an information perspective. Saf. Sci. 112 (2019), 38–47. https://doi.org/10.1016/j.ssci.2018.09.014.
- Silva, I.O., 2009. Distribuição da Vazão Fluvial no Estuário do Rio Amazonas. In: Master's Thesis, Universidade Federal do Rio de Janeiro. Brasil, Rio de Janeiro
- Spaulding, M.L.A., 1988. State-of-the-art review of oil spill trajectory and fate modeling. Oil Chem. Pollut. 4, 39–55. https://doi.org/10.1016/S0269-8579(88)80009-1.
- Torres, A.M., El-Robrini, M., Costa, W.J.P., 2018. Panorama da erosão costeira- Amapá. In: Muehe, D. (Ed.), Panorama da Erosão Costeira no Brasil, 2018. Ministério do Meio Ambiente, Macapá, Brasil, pp. 19–63.
- Toz, A., Koseoglu, B., Sakar, C., 2016. Numerical modelling of oil spill in New York Bay. Arch. Environ. Prot. 42 https://doi.org/10.1515/aep-2016-0037.
- Uğurlu, Ö., Köse, E., Yildirim, Ü., Yüksekyildiz, E., 2015. Marine accident analysis for collision and grounding in oil tanker using FTA method. Marit. Policy Manag. 42 (2), 163–185. https://doi.org/10.1080/03088839.2013.856524.
- UNCTAD United Nations Conference on Trade and Development, secretariat, 2008. Review of Maritime Transport. UNCTAD/RMT/2008 (Sales No. E.08.II.D.26), United Nations Publication. https://unctad.org/system/files/official-document/rmt200 8 en.pdf.
- Vairo, T., Quagliati, M., Del Giudice, T., Barbucci, A., Fabiano, B., 2016. From land- to water-use-planning: a consequence based case-study related to cruise ship risk. Safety Sci. https://doi.org/10.1016/j.ssci.2016.03.024.
- Valerio, A.M., Kampel., M., Vantrepotte, V., Ward, N.D., Sawakuchi, H.O., Less, D.F.S., Neu, V., Cunha, A.C., Richey, J.E., 2018. Using CDOM optical properties for estimating DOC concentrations and pCO in the Lower Amazon River. Opt. Express 26, A657–A677. https://doi.org/10.1364/OE.26.00A657.
- Van Dorp, J.R., Merrick, J.R.W., 2011. On a risk management analysis of oil spill risk using maritime transportation system simulation. Ann. Oper. Res. 187 (1), 249–277. https://doi.org/10.1007/s10479-009-0678-1.
- Vieira, A.A.S., Hamacher, S., Santos, I.M., 2017. Dimensionamento da frota de navios de derivados claros para cabotagem: proposta de modelo de otimização. Transportes 25 (3), 75–89. https://doi.org/10.14295/transportes.v25i3.1315.
- Ward, N.D., Keil, R.G., Medeiros, P.M., Brito, D.C., Cunha, A.C., Dittmar, T., Yager, P.L., Krusche, A.V., Richey, J.E., 2013. Degradation of terrestrially derived macromolecules in the Amazon River. Nat. Geosci. 6, 530–533. https://doi.org/ 10.1038/ngen1817.
- Ward, N.D., Bianchi, T.S., Sawakuchi, H.O., Gagne-Maynard, W., Cunha, A.C., Brito, D. C., Neu, V., de Matos, A., da Silva, V.R., Krusche, A.V., Richey, J.E., Keil, R.G., 2016. The reactivity of plant-derived organic matter and the potential importance of priming effects along the lower Amazon River. J. Geophys. Res. Biogeosci. 121, 1522–1539. https://doi.org/10.1002/2016JG003342.
- Xu, Q., Wang, N., 2014. A survey on ship collision risk evaluation. Traffic management review. Promet Traffic Transp. 26 (6), 475–486. https://doi.org/10.7307/ptt. 1006/1006
- Yoo, Y., Kim, T.G., 2019. An improved ship collision risk evaluation method for Korea maritime safety audit considering traffic flow characteristics. J. Mar. Sci. Eng. 7, 448. https://doi.org/10.3390/jmse7120448.
- Zamboni, A., Tavares, A.R., Nicolodi, J.L., Carvalho, L.R. de, Cabral, A., Muehe, D., Silva, G.H. da, Jablonski, S., Sakata, F., Menecucc, T.M., Fecarotta, M. da C.S., Cossia, D., 2004. Especificações e normas técnicas para elaboração de cartas de sensibilidade ambiental para derramamentos de óleo. Ministério do Meio Ambiente (MMA). Brasília, DF, Brasíl.
- Zanāo, L.R., Dos Santos, B.C.D.B., Sequinel, R., Flumignan, D.L., De Oliveira, J.E., 2018. Prediction of Relative Density, Distillation Temperatures, Flash Point, and Cetane Number of S500 Diesel Oil Using Multivariate Calibration of Gas Chromatographic Profiles Energy & Fuels, 32 (8), pp. 8108–8114. https://doi.org/10.1021/acs. energyfuels.8b01295.